

Tracing the source of nitrate ~~enriched~~ in a forested stream showing elevated concentrations during storm events

Weitian Ding¹, Urumu Tsunogai¹, Fumiko Nakagawa¹, Takashi Sambuichi¹, Hiroyuki Sase², Masayuki Morohashi², Hiroki Yotsuyanagi²

¹ Graduate School of Environmental Studies, Nagoya University, Furo-cho, Chikusa-ku, Nagoya 464-8601, Japan

²Asia Center for Air Pollution Research, 1182 Sowa, Nishi-ku, Niigata-shi, Niigata 950-2144, Japan

Corresponding author: Weitian Ding, Email: ding.weitian.v2@s.mail.nagoya-u.ac.jp
dingweitian@nagoya-u.jp

1 Abstract

2 To clarify the source of nitrate increased during storm events in a temperate forested
3 streams, we monitored temporal variation in the concentrations and stable isotopic
4 compositions including $\Delta^{17}\text{O}$ of stream nitrate in a forested catchment (KJ catchment,
5 Japan) during three storm events I, II, and III (summer). The stream showed significant
6 increase temporal variation in nitrate concentration, - from 24.7 μM to 122.6 μM , from
7 28.7 μM to 134.1 μM , and from 46.6 μM to 114.5 μM during the storm events I, II, and
8 III, respectively. On the other hand, the isotopic compositions ($\delta^{15}\text{N}$, $\delta^{18}\text{O}$, and $\Delta^{17}\text{O}$)
9 of stream nitrate showed a decrease in accordance with the increase in the stream nitrate
10 concentration, from +2.5 ‰ to -0.1 ‰, from +3.0 ‰ to -0.5 ‰, and from +3.5 ‰ to
11 -0.1 ‰ for $\delta^{15}\text{N}$, from +3.1 ‰ to -3.4 ‰, from +2.9 ‰ to -2.5 ‰, and from +2.1 ‰
12 to -2.3 ‰ for $\delta^{18}\text{O}$, and from +1.6 ‰ to +0.3 ‰, from +1.4 ‰ to +0.3 ‰, and from
13 +1.2 ‰ to +0.5 ‰ for $\Delta^{17}\text{O}$ during the storm events I, II, and III, respectively. Besides,
14 we found strong linear relationships between the isotopic compositions (~~$\delta^{15}\text{N}$, $\delta^{18}\text{O}$, and~~
15 $\Delta^{17}\text{O}$) of stream nitrate and the reciprocal of stream nitrate concentrations during each
16 storm event, implying that the temporal variation in the stream nitrate can be explained
17 by simple mixing between two distinctive endmembers of nitrate having different
18 isotopic compositions. Furthermore, we found that both concentrations and the isotopic
19 compositions of soil nitrate obtained in the riparian zone of the stream were plotted on
20 the nitrate-enriched extension of the linear relationship. We conclude that the soil nitrate

21 in the riparian zone was primarily responsible for the increase in stream nitrate during
22 the storm events. In addition, we found that the concentration of unprocessed
23 atmospheric nitrate in the stream was stable at $1.6 \pm 0.4 \mu\text{M}$, $1.8 \pm 0.4 \mu\text{M}$, and $2.1 \pm$
24 $0.4 \mu\text{M}$ during the storm events I, II, and III, respectively, irrespective to the significant
25 variations in the total nitrate concentration. We conclude that the storm events have
26 little impacts on the concentration of unprocessed atmospheric nitrate in the stream and
27 thus the annual export flux of unprocessed atmospheric nitrate relative to the annual
28 deposition flux can be a robust index to evaluate nitrogen saturation in —forested
29 catchments, irrespective to the variation in the number of storm events and/or the
30 variation in the elapsed time from storm events to sampling.

31

32 **1 Introduction**

33 Nitrate is ~~a—representative~~an important nitrogenous nutrient in biosphere.
34 Traditionally, forested ecosystems have been considered nitrogen limited (Vitousek and
35 Howarth, 1991). Due to the elevated loading of nitrogen through atmospheric
36 deposition, however, some forested ecosystems become nitrogen saturated (Aber et al.,
37 1989), from which elevated levels of nitrate are exported (Mitchell et al., 1997;
38 Peterjohn et al., 1996). In addition, sudden increase in the concentration of nitrate in
39 response to storm events has been reported in forested streams worldwide (Aguilera
40 and Melack, 2018; Creed et al., 1996; Kamisako et al., 2008; McHale et al., 2002),
41 which further enhanced nitrate export from forested ecosystems.

42 Such excessive leaching of nitrate from forested catchment degrades water quality
43 and cause eutrophication in downstream areas (Galloway et al., 2003; Paerl and
44 Huisman, 2009). Thus, tracing the source of nitrate increase during storm events in
45 forested streams is important for sustainable forest management, especially for ~~those~~the
46 nitrogen-saturated forested ecosystems.

47 As for the source of nitrate that was added to stream during storm events, either of
48 the two possible sources have been assumed in past studies; (1) atmospheric nitrate
49 ($\text{NO}_3^-_{\text{atm}}$) in rainwater originally and being supplied directly to stream water (Inamdar
50 and Mitchell, 2006) ~~through the overland flow~~ (Kaushal et al., 2011; Sebestyen et al.,
51 2014), and (2) soil nitrate originally and being supplied to stream water by the flushing
52 effects on soils (Creed et al., 1996; Ocampo et al., 2006). Nevertheless, monitoring the
53 variation in nitrate concentration, it is difficult to clarify the primary source of nitrate
54 that increases during storm events.

55 The natural stable isotopic composition of nitrate has been widely applied to clarify
56 the sources of nitrate in natural freshwater systems (Burns and Kendall, 2002; Durka et
57 al., 1994; Kendall et al., 2007). In particular, triple oxygen isotopic compositions of
58 nitrate ($\Delta^{17}\text{O}$) have been used in recent days as a conservative tracer of $\text{NO}_3^-_{\text{atm}}$
59 deposited onto a forested catchment (Inoue et al., 2021; Michalski et al., 2004;
60 Nakagawa et al., 2018; Tsunogai et al., 2014), showing distinctively different $\Delta^{17}\text{O}$ from
61 that of remineralized nitrate ($\text{NO}_3^-_{\text{re}}$), derived from organic nitrogen through general
62 chemical reactions, including microbial N mineralization and microbial nitrification.

63 While $\text{NO}_3^-_{\text{re}}$, the oxygen atoms of which are derived from either terrestrial O_2 or H_2O
64 through microbial processing (i.e., nitrification), always shows the relation close to the
65 “mass-dependent” relative relation between $^{17}\text{O}/^{16}\text{O}$ ratios and $^{18}\text{O}/^{16}\text{O}$ ratios; $\text{NO}_3^-_{\text{atm}}$
66 displays an anomalous enrichment in ^{17}O reflecting oxygen atom transfers from
67 atmospheric ozone (O_3) during the conversion of NO_x to $\text{NO}_3^-_{\text{atm}}$ (Alexander et al.,
68 2009; Michalski et al., 2003; Morin et al., 2011; Nelson et al., 2018). As a result, the
69 $\Delta^{17}\text{O}$ signature defined by the following equation (Kaiser et al., 2007) enables us to
70 distinguish $\text{NO}_3^-_{\text{atm}}$ ($\Delta^{17}\text{O} > 0$) from $\text{NO}_3^-_{\text{re}}$ ($\Delta^{17}\text{O} = 0$):

$$71 \quad \Delta^{17}\text{O} = \frac{1 + \delta^{17}\text{O}}{(1 + \delta^{18}\text{O})^\beta} - 1 \quad (1)$$

72 where the constant β is 0.5279 (Kaiser et al., 2007), $\delta^{18}\text{O} = R_{\text{sample}}/R_{\text{standard}} - 1$ and R is
73 the $^{18}\text{O}/^{16}\text{O}$ ratio (or the $^{17}\text{O}/^{16}\text{O}$ ratio in the case of $\delta^{17}\text{O}$ or the $^{15}\text{N}/^{14}\text{N}$ ratio in the case
74 of $\delta^{15}\text{N}$) of the sample and each standard reference material. In addition, $\Delta^{17}\text{O}$ is almost
75 stable during “mass-dependent” isotope fractionation processes within terrestrial
76 ecosystems. Therefore, while the $\delta^{15}\text{N}$ or $\delta^{18}\text{O}$ signature of $\text{NO}_3^-_{\text{atm}}$ can be overprinted
77 by the biological processes subsequent to deposition, $\Delta^{17}\text{O}$ can be used as a robust tracer
78 of unprocessed $\text{NO}_3^-_{\text{atm}}$ to reflect its accurate mole fraction within total NO_3^- , regardless
79 of the progress of the partial metabolism (partial removal of nitrate through
80 denitrification and assimilation) subsequent to deposition (Michalski et al., 2004;
81 Nakagawa et al., 2013, 2018; Tsunogai et al., 2011, 2014, 2018).

82 While the variation in the $\delta^{18}\text{O}$ and/or $\Delta^{17}\text{O}$ of nitrate in forested streams during storm
83 events have been reported in past studies (Sebestyen et al., 2019; Sabo et al., 2016;

84 Buda and Dewalle. 2009), the temporal resolutions of sampling were less than 10
85 times/day during storm events and the source of the stream nitrate increased during
86 storm events has not been clarified yet.

87 In this study, we determined the temporal variation in the concentrations and the
88 isotopic compositions ($\delta^{15}\text{N}$, $\delta^{18}\text{O}$, and $\Delta^{17}\text{O}$) of stream nitrate at once every hour during
89 storm events in a forested catchment to ~~by using the stable isotopes including $\Delta^{17}\text{O}$ of~~
90 ~~nitrate as tracers, we clarified~~ clarify (1) the source of nitrate in a forested stream that
91 was added during storm events, and (2) the temporal variation in the concentration of
92 $\text{NO}_3^-_{\text{atm}}$ in response to storm events. In addition, the impacts of storm events on the
93 index of nitrogen saturation lately proposed by Nakagawa et al. (2018) were discussed.

94

95 **2 Methods**

96 2.1 Study site

97 As for the studying field to trace the source of stream nitrate during storm events, we
98 chose Kajikawa forested catchment (KJ catchment) in Japan, in which several past
99 studies had been done to clarify the temporal variation in the concentration of stream
100 nitrate and the status of nitrogen saturation (Kamisako et al., 2008; Nakagawa et al.,
101 2018; Sase et al., 2021). This is a small, forested catchment (3.84 ha) located in the
102 northern part of Shibata City, Niigata Prefecture, along the coast of Sea of Japan (Fig.
103 1a). The KJ catchment predominantly slopes towards the west-northwest, with a mean
104 slope of 36° , and the elevation ranges from 60 to 170 m above sea level (Fig. 1b). The

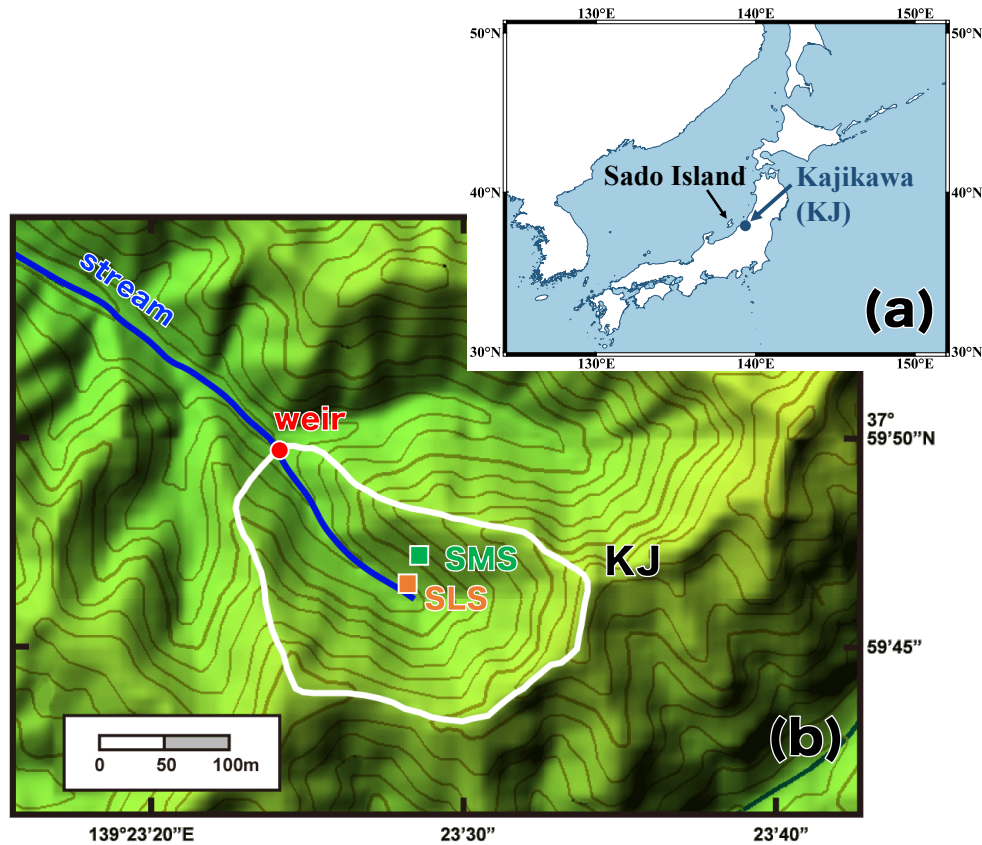
105 catchment is fully covered by Japanese cedars (*Cryptomeria japonica* D. Don) that were
106 approximately 46 years old in 2018 (Sase et al., 2021). The parent material is
107 granodiorite and brown forest soils (Cambisols) have developed in this area (Kamisako
108 et al., 2008; Sase et al., 2008). The lowest, highest, and mean monthly temperatures
109 recorded at the nearest meteorological station (Nakajo station) were 1.0 °C (in February),
110 27.9 °C (in August), and 14.5 °C, respectively, from 2017/5 to 2020/3. The annual mean
111 precipitation was around 2500 mm, approximately 17% of which occurred during
112 spring (from March to May), approximately 20% during summer (from June to August),
113 approximately 28% during fall (from September to November), and approximately 35%
114 during winter (from December to February). The catchment usually experiences
115 snowfall from late December to March.

116 From 2003 to 2005, Kamisako et al. (2008) determined temporal variation in the
117 concentration of Ca^{2+} , Mg^{2+} , Cl^- , and NO_3^- eluted from the catchment via a stream at
118 intervals of 1 to 3 hour for 2 to 3 days on each and found that significant increase in the
119 stream nitrate concentration during storm events, from less than 30 μM to more than
120 120 μM . On the basis of the observed nitrate enrichment in the stream water, they
121 concluded that atmospheric nitrogen inputs exceeded the biological demand at the
122 catchment and proposed that the KJ catchment was under nitrogen saturation.
123 Nakagawa et al. (2018) determined temporal variation in the concentrations and stable
124 isotopic compositions ($\delta^{15}\text{N}$, $\delta^{18}\text{O}$, and $\Delta^{17}\text{O}$) of both stream nitrate and soil nitrate for
125 two years (from 2012/12 to 2014/12) and concluded that nitrate in the groundwater of

126 the catchment was the major source of nitrate in the stream water during the base flow
127 periods. Additionally, Nakagawa et al. (2018), who proposed the export flux of NO_3^- -atm
128 (M_{atm}) relative to the deposition flux of NO_3^- -atm (D_{atm}) can be an alternative, more robust
129 index for nitrogen saturation in temperate forested catchments, clarified that ~~the~~
130 export flux of unprocessed atmospheric nitrate M_{atm} relative to the deposition flux of
131 atmospheric nitrate D_{atm} ratio in the KJ catchment ~~($M_{\text{atm}}/D_{\text{atm}}$)~~ was larger (9.4 %) than
132 the other catchments they studied simultaneously (6.5 % and 2.6 % ~~respectively~~), which
133 also ~~implied the KJ catchment was under the nitrogen saturation and proposed that the~~
134 ~~$M_{\text{atm}}/D_{\text{atm}}$ ratio can be used as the index of nitrogen saturation.~~ Moreover, Sase et al.
135 (2021) reported the nitrate concentration of the stream has been increasing in recent
136 years, which implies that nitrogen saturation is still ongoing in the forest.

137

138



139 **Figure. 1** A map showing the locations of the studied Kajikawa (KJ) catchment in Japan
 140 (a) and a colored altitude map of the KJ catchment (b) (modified after Nakagawa et al.
 141 2018). The white line denotes the whole catchment area, and the red circle denotes the
 142 position of the weir where the stream water was sampled. The orange (SLS) and green
 143 (SMS) ~~circles~~ ~~squares~~ denote the sampling stations of soil water in the riparian and
 144 upland zone, respectively, in the past study (Nakagawa et al., 2018).

145

146 2.2 Discharge rates and weather information

147 A V-notch weir (half angle: 30°) and a partial flume were installed at the bottom of
 148 the catchment (Fig. 1b), where the discharge rates were determined. The weather
 149 information including the precipitation monitored by Japan Meteorological Agency at
 150 the nearest station of KJ catchment (Nakajo station; 38°04'60" N, 139°23'30" E) was

151 used for that in the KJ catchment. Because the accumulated snow was not monitored
152 in Nakajo station, however, those monitored at the Niigata station (37°53'60" N,
153 139°01'10" E) was used instead.

154

155 2.3 Sampling

156 In this study, the concentrations and stable isotopic compositions ($\delta^{15}\text{N}$, $\delta^{18}\text{O}$, and
157 $\Delta^{17}\text{O}$) of stream nitrate eluted from the KJ catchment were monitored every month
158 ~~additionally~~ for more than 2 years (routine observation). Additionally, during storm
159 events, the same parameters were monitored every hour for 1 day (intensive
160 observation). Stream water was sampled at the weir located on the outlet of the KJ
161 catchment (Fig. 1b). Routine observation was performed manually using bottles at the
162 weir approximately once a month from 2017/5 to 2020/3. Intensive observation was
163 conducted during the three storm events I, II, and III (2019/8/22, 2019/10/12, and
164 2020/9/13, respectively), where the water samples were collected at intervals of 1 hour
165 over 24 hours using an automatic water sampler (SIGMA 900, Hach, USA). In this
166 study, 0.5 or 2 L polyethylene bottles washed using chemical detergents were rinsed at
167 least three times using deionized water and dried in the laboratory before being used to
168 store the water samples.

169

170 2.4 Analysis

171 Samples of stream water for the routine observation were transported to the

172 laboratory within 1 hour after being collected manually. Samples for the intensive
173 observation were transported within ~~1 or 2 weeks~~ 12 days after completion of the
174 automatic sampling ([Table 1](#)). All samples were passed through a membrane filter (pore
175 size 0.45 μm) and stored in a refrigerator (4 $^{\circ}\text{C}$) ~~prior to~~ until their chemical analysis.

176 The concentrations of nitrate were measured by ion chromatography (DX-500;
177 Dionex Inc., USA). To determine the stable isotopic compositions of nitrate in the
178 stream water samples, nitrate in each sample was chemically converted to N_2O using a
179 method originally developed to determine the $^{15}\text{N}/^{14}\text{N}$ and $^{18}\text{O}/^{16}\text{O}$ ratios of seawater
180 and freshwater nitrate (McIlvin and Altabet, 2005) that was later modified (Konno et
181 al., 2010; Tsunogai et al., 2011; Yamazaki et al., 2011). In brief, 11 mL of each sample
182 solution was pipetted into a vial with a septum cap. Then, 0.5 g of spongy cadmium
183 was added, followed by 150 μL of a 1 M NaHCO_3 solution. The sample was then shaken
184 for 18-24 h at a rate of 2 cycles s^{-1} . Then, the sample solution (10 mL) was decanted
185 into a different vial with a septum cap. After purging the solution using high-purity
186 helium, 0.4 mL of an azide-acetic acid buffer, which had also been purged using high-
187 purity helium, was added. After 45 min, the solution was alkalized by adding 0.2 mL
188 of 6 M NaOH .

189 Then, the stable isotopic compositions ($\delta^{15}\text{N}$, $\delta^{18}\text{O}$, and $\Delta^{17}\text{O}$) of the N_2O in each vial
190 were determined using the continuous-flow isotope ratio mass spectrometry (CF-IRMS)
191 system at Nagoya University. The analytical procedures performed using the CF-IRMS
192 system were the same as those detailed in previous studies (Hirota et al., 2010; Komatsu

193 et al., 2008). The obtained values of $\delta^{15}\text{N}$, $\delta^{18}\text{O}$, and $\Delta^{17}\text{O}$ for the N_2O derived from the
194 nitrate in each sample were compared with those derived from our local laboratory
195 nitrate standards to calibrate the values of the sample nitrate to an international scale
196 and to correct for both isotope fractionation during the chemical conversion to N_2O and
197 the progress of oxygen isotope exchange between the nitrate derived reaction
198 intermediate and water (ca. 20 %). The local laboratory nitrate standards used for the
199 calibration had been calibrated using the internationally distributed isotope reference
200 materials (USGS-34 and USGS-35). In this study, we adopted the internal standard
201 method (Nakagawa et al., 2013, 2018; Tsunogai et al., 2014) to calibrate the stable
202 isotopic compositions of sample nitrate. In order to calibrate the differences in $\delta^{18}\text{O}$ of
203 H_2O between the samples and those our local laboratory nitrate standards were added
204 for calibration, the $\delta^{18}\text{O}$ values of H_2O in the samples were analyzed as well (Tsunogai
205 et al., 2010, 2011, 2014).

206 To determine whether the conversion rate from nitrate to N_2O was sufficient, the
207 concentration of nitrate in the samples was determined each time we analyzed the
208 isotopic composition using CF-IRMS based on the N_2O^+ or O_2^+ outputs. We adopted
209 the $\delta^{15}\text{N}$, $\delta^{18}\text{O}$, and $\Delta^{17}\text{O}$ values only when the concentration measured via CF-IRMS
210 correlated with the concentration measured via ion chromatography prior to isotope
211 analysis within a difference of 10 %.

212 Three kinds of the local laboratory nitrate standards were used to determine the
213 isotopic compositions of stream nitrate, which had been named to be GG01 ($\delta^{15}\text{N} = -$

214 3.07 ‰, $\delta^{18}\text{O} = +1.10$ ‰, and $\Delta^{17}\text{O} = 0$ ‰), HDLW02 ($\delta^{15}\text{N} = +16.11$ ‰, $\delta^{18}\text{O} = +22.$
215 20 ‰), and NF ($\delta^{18}\text{O} = +54.14$ ‰, $\Delta^{17}\text{O} = +19.16$ ‰). Both GG01 and HDLW02 were
216 used to determine $\delta^{15}\text{N}$ and $\delta^{18}\text{O}$ of stream nitrate, and both GG01 and NF were used
217 to determine $\Delta^{17}\text{O}$ of stream nitrate. The standard errors of the mean in the isotopic
218 compositions ($\delta^{15}\text{N}$, $\delta^{18}\text{O}$, and $\Delta^{17}\text{O}$) determined through repeated measurements on
219 GG01 (n = 3), were ± 0.17 ‰ for $\delta^{15}\text{N}$, ± 0.25 ‰ for $\delta^{18}\text{O}$, and ± 0.10 ‰ for $\Delta^{17}\text{O}$, during
220 the measurements in this study. We repeated the analysis of $\delta^{15}\text{N}$, $\delta^{18}\text{O}$, and $\Delta^{17}\text{O}$ values
221 for each sample at least three times to attain high precision. All samples had a nitrate
222 concentration of greater than 10 μM , which corresponded to a nitrate quantity greater
223 than 100 nmol in a 10 mL sample. Thus, all isotope values presented in this study have
224 an error (standard error of the mean) better than ± 0.2 ‰ for $\delta^{15}\text{N}$, ± 0.3 ‰ for $\delta^{18}\text{O}$, and
225 ± 0.1 ‰ for $\Delta^{17}\text{O}$.

226 Nitrite (NO_2^-) in the samples interferes with the final N_2O produced from nitrate
227 because the chemical method also converts NO_2^- to N_2O (McIlvin and Altabet, 2005).
228 Therefore, it is sometimes necessary to remove NO_2^- prior to converting nitrate to N_2O .
229 However, in this study, all the stream and soil water samples analyzed for stable isotopic
230 composition had NO_2^- concentrations lower than the detection limit (0.05 μM).
231 Because the minimum nitrate concentration in the samples was 24.7 μM in this study,
232 the ratios of NO_2^- to nitrate in the samples must be less than 0.2 %. Thus, we skipped
233 the processes for removing NO_2^- .

234

235 2.5 Calculating of the concentration of unprocessed $\text{NO}_3^-_{\text{atm}}$ in stream water

236 The $\Delta^{17}\text{O}$ data of nitrate in each sample can be used to estimate the concentration of
237 $\text{NO}_3^-_{\text{atm}}$ ($[\text{NO}_3^-_{\text{atm}}]$) in the stream water samples by applying Eq. (2):

238
$$[\text{NO}_3^-_{\text{atm}}]/[\text{NO}_3^-] = \Delta^{17}\text{O}/\Delta^{17}\text{O}_{\text{atm}} \quad (2)$$

239 where $[\text{NO}_3^-_{\text{atm}}]$ and $[\text{NO}_3^-]$ denote the concentration of $\text{NO}_3^-_{\text{atm}}$ and nitrate (total) in
240 each water sample, respectively, and $\Delta^{17}\text{O}_{\text{atm}}$ and $\Delta^{17}\text{O}$ denote the $\Delta^{17}\text{O}$ values of
241 $\text{NO}_3^-_{\text{atm}}$ and nitrate (total) in the stream water sample, respectively. In this study, we
242 used the average $\Delta^{17}\text{O}$ value of $\text{NO}_3^-_{\text{atm}}$ determined at the nearby Sado-Seki monitoring
243 station during the observation from April 2009 to March 2012 ($\Delta^{17}\text{O}_{\text{atm}} = +26.3 \text{ ‰}$;
244 Tsunogai et al., 2016) for $\Delta^{17}\text{O}_{\text{atm}}$ in Eq. (2) to estimate $[\text{NO}_3^-_{\text{atm}}]$ in the stream. We
245 allow for an error range in of 3 ‰ in $\Delta^{17}\text{O}_{\text{atm}}$, in which the factor changes in $\Delta^{17}\text{O}_{\text{atm}}$
246 from +26.3 ‰ caused by both areal and seasonal variation in the $\Delta^{17}\text{O}$ values of $\text{NO}_3^-_{\text{atm}}$
247 have been considered (Nakagawa et al., 2018; Tsunogai et al., 2016).

248

249 **Table 1.** Information on the samples taken during the intensive observation.

<u>Storm event</u>	<u>Start time</u>	<u>End time</u>	<u>Date of filtration</u>	<u>Maximum period of storage without filtration</u>
<u>I</u>	<u>2019/8/22 16:00</u>	<u>2019/8/23 15:00</u>	<u>2019/8/29</u>	<u>7 days</u>
<u>II</u>	<u>2019/10/12 15:00</u>	<u>2019/10/13 14:00</u>	<u>2019/10/23</u>	<u>11 days</u>
<u>III</u>	<u>2020/9/13 11:00</u>	<u>2020/9/14 10:00</u>	<u>2020/9/25</u>	<u>12 days</u>

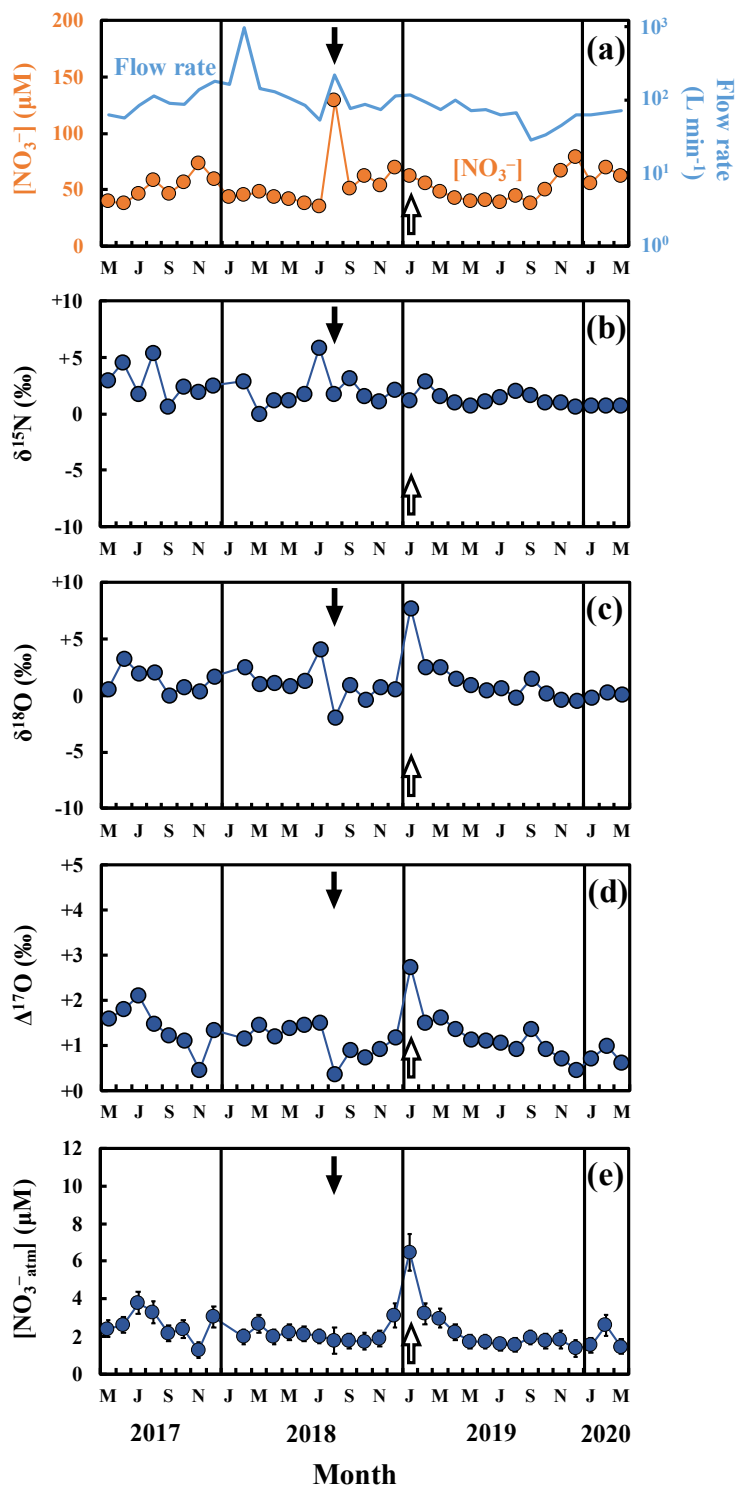
250

251 **3 Results**

252 3.1 Variation during the routine observation

253 During the routine observation, the concentrations of stream nitrate ranged from
254 35.7 μM to 129.3 μM with the flux-weighted average concentration of 55.6 μM (Fig.
255 2a), showing little temporal changes from that determined during the past observations
256 from 2013 to 2014 at the same catchment (58.4 μM ; Nakagawa et al., 2018). The
257 variation range also agreed with the past observation done in the same catchment
258 (Kamisako et al., 2008), except for the extraordinarily large concentration (129.3 μM)
259 recorded on 2018/8/31, which exceeded the 2σ of the whole variation range of stream
260 nitrate of our routine observation (Fig. 2a). We will discuss the reason in section 4.21.

261 The stable isotopic compositions of stream nitrate during the routine observation
262 ranged from +0.1 ‰ to +5.9‰ for $\delta^{15}\text{N}$ (Fig. 2b), from -1.9 ‰ to +7.7 ‰ for $\delta^{18}\text{O}$ (Fig.
263 2c), and from +0.4 ‰ to +2.7 ‰ for $\Delta^{17}\text{O}$ (Fig. 2d), while showing little seasonal
264 variation. The flux-weighted averages for the $\delta^{15}\text{N}$, $\delta^{18}\text{O}$, and $\Delta^{17}\text{O}$ values of nitrate
265 were +2.0 ‰, +1.1 ‰, and +1.1 ‰, respectively. Except for the extraordinarily large
266 $\delta^{18}\text{O}$ and $\Delta^{17}\text{O}$ values we found on 2019/1/31 ($\delta^{18}\text{O} = +7.7$ ‰ and $\Delta^{17}\text{O} = +2.7$ ‰)
267 (Figs. 2c and 2d), the values are typical for stream nitrate eluted from temperate forested
268 catchments (Hattori et al., 2019; Huang et al., 2020; Nakagawa et al., 2013, 2018; Riha
269 et al., 2014; Sabo et al., 2016; Tsunogai et al., 2014, 2016). On the other hand, the data
270 recorded on 2019/1/31 exceeded the 2σ variation range of the whole $\delta^{18}\text{O}$ and $\Delta^{17}\text{O}$
271 data. We will discuss the reason in section 4.32.



273 **Figure 2.** Temporal variations in the concentrations of nitrate (orange circles) and the
 274 flow rates (blue line) in the stream water during the routine observation (a), together
 275 with those of the values of $\delta^{15}\text{N}$ (b), $\delta^{18}\text{O}$ (c), $\Delta^{17}\text{O}$ (d) of nitrate, and the concentrations

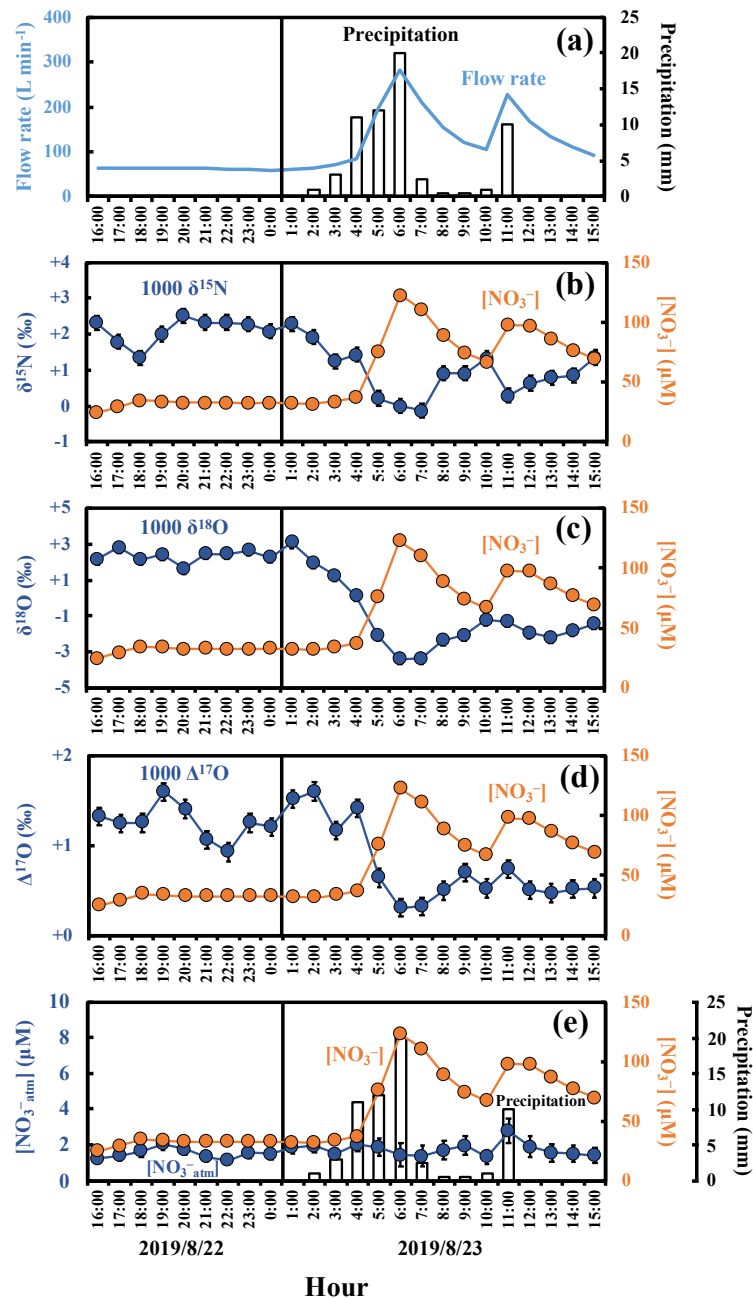
276 of unprocessed atmospheric nitrate ($[\text{NO}_3^-_{\text{atm}}]$) (e) in the stream water (blue circles).
277 The black and white arrows in the figures indicate the sampling that took place on
278 2018/8/31 and 2019/1/31, respectively. The error bars smaller than the sizes of the
279 symbols are not presented.

280

281 3.2 Variation in response to the storm events

282 During the intensive observations made in response to the storm events, the
283 concentration of stream nitrate showed significant short-term variation, from 24.7 μM
284 to 122.6 μM , from 28.7 μM to 134.1 μM , and from 46.6 μM to 114.5 μM during the
285 storm events I, II, and III, respectively, with the minimum recorded just before the
286 beginning of each storm event and the maximum recorded when the flow rate was close
287 to the maximum within each storm event (Figs. 3 and S1). Similar increase in the
288 concentrations of stream nitrate in accordance with the increase in the flow rate during
289 storm events have been reported in many past studies (e.g. Burns et al., 2019; Chen et
290 al., 2020; Kamisako et al., 2008; Christopher et al., 2008). Especially, Kamisako et al.
291 (2008), who monitored temporal changes in the concentration of stream nitrate in the
292 same KJ catchment from 2003 to 2005 and found 11 nitrate increase events in
293 accordance with the increase in the flow rate, reported the largest concentration of
294 stream nitrate during the events to be 120 μM . –The pattern and range of the short-
295 term variation of the stream nitrate concentration during the three storm events were
296 also consistent with the past study ~~done in the same catchment~~ (Kamisako et al., 2008).

297 The stable isotopic compositions of stream nitrate during the three storm events also
298 showed significant temporal variation, from -0.1‰ to $+2.5\text{‰}$, from -0.5‰ to $+3.0\text{‰}$,
299 and from -0.1‰ to $+3.5\text{‰}$ for $\delta^{15}\text{N}$ (Figs. 3b, S1b, and S1g), from -3.4‰ to $+3.1\text{‰}$,
300 from -2.5‰ to $+2.9\text{‰}$, and from -2.3‰ to $+2.1\text{‰}$ for $\delta^{18}\text{O}$ (Figs. 3c, S1c, and S1h),
301 and from $+0.3\text{‰}$ to $+1.6\text{‰}$, from $+0.3\text{‰}$ to $+1.4\text{‰}$, and from $+0.5\text{‰}$ to $+1.2\text{‰}$ for
302 $\Delta^{17}\text{O}$ (Figs. 3d, S1d, and S1i), with minimum values observed when the concentration
303 of stream nitrate was at maximum and maximum values observed when the
304 concentration of stream nitrate was at a minimum.



306 **Figure. 3** Temporal variations in the amount of precipitation (bar chart) and flow rates
 307 (blue line) of the stream water (blue line) during storm events I (a), together with those
 308 in the concentrations of nitrate (orange circles) (b-e), the values of $\delta^{15}\text{N}$ (b), $\delta^{18}\text{O}$ (c),
 309 $\Delta^{17}\text{O}$ (d) of nitrate, and $[\text{NO}_3^-]_{\text{atm}}$ (e) in the stream water (blue circles). The error bars
 310 smaller than the sizes of the symbols are not presented.

311

312 **4 Discussion**

313 4.1 Possible alterations to the concentration and isotopic compositions of stream nitrate
314 during the storage period in the automatic sampler used for the intensive
315 observations~~4.1 Primary source of nitrate increased during storm events~~

316 During the intensive observations, the stream water samples were stored in bottles of
317 the automatic sampler. The storage periods until filtration were ranged from 7 (storm
318 event I) to 12 days (storm event III) (Table 1). While the automatic sampler was
319 surrounded by ferns and the other understory vegetations to minimize the possible
320 alterations on the samples, progress of biogeochemical reactions such as nitrification,
321 denitrification, and assimilation could alter the concentration and isotopic compositions
322 ($\delta^{15}\text{N}$, $\delta^{18}\text{O}$, and $\Delta^{17}\text{O}$) of stream nitrate during the storage period. Above all, possible
323 increase in soil water input into the stream water that is enriched with organic matters
324 during a storm event could enhance nitrification during the storage period and could
325 increase the concentration of nitrate in the stream water samples taken by using the
326 automatic sampler.

327 As a result, we discussed the possible alteration of the concentration and isotopic
328 compositions during the storage for the samples taken by using the automatic sampler
329 and concluded that the alterations during the storage in the automatic sampler were
330 minor in the samples. The details are described in Appendix A.

331 ~~4.1~~ 4.2 Primary source of nitrate increased during storm events

332 The striking feature of the observed short-term variation was that all the stable
333 isotopic compositions ($\delta^{15}\text{N}$, $\delta^{18}\text{O}$, and $\Delta^{17}\text{O}$) varied in response to the variation in the
334 nitrate concentration throughout the three storm events (Figs. 3 and S1). The result
335 implied that the source of increased nitrate during the storm events were different from
336 that during the base flow period.

337 As a result, the stable isotopic compositions ($\delta^{15}\text{N}$, $\delta^{18}\text{O}$, and $\Delta^{17}\text{O}$) of stream
338 nitrate were plotted as the functions of the reciprocal of the stream nitrate
339 concentration ($1/[\text{NO}_3^-]$) for each storm event (Fig. 4). All the stable isotopic
340 compositions of stream nitrate ($\delta^{15}\text{N}$, $\delta^{18}\text{O}$, and $\Delta^{17}\text{O}$) showed strong linear
341 relationships ($R^2 > 0.5$; $p < 0.001$) with the reciprocal of concentrations. The linear
342 relationships strongly suggest mixing between two endmembers with distinctively
343 different isotopic signatures (e.g. Keeling, 1958). The observed strong linear
344 relationships not only in the $\Delta^{17}\text{O}$ of stream nitrate (Figs. 4g, 4h, and 4i), which is
345 stable during the progress of partial removal reactions such as denitrification or
346 assimilation, but also in the $\delta^{15}\text{N}$ and $\delta^{18}\text{O}$ of stream nitrate (Figs. 4a-4f), which
347 should be altered during the progress of the partial removal reactions, also implied
348 that the progress of denitrification or assimilation in bottles of the automatic sampler
349 during the storage period without filtration were minor in the samples.

350 The nitrate-depleted endmember must be the source of stream nitrate during the
351 base flow period prior to each storm event. On the other hand, the nitrate-enriched
352 endmember represents the source of nitrate that was added during the storm events.

353 Atmospheric nitrate ($\text{NO}_3^-_{\text{atm}}$) dissolved in rainwater was one of the possible
354 sources of nitrate enriched during the storm events ([Inamdar and Mitchell, 2006](#))
355 ([Kaushal et al., 2011](#); [Sebestyén et al., 2014](#)). While the $\text{NO}_3^-_{\text{atm}}$ showed the $\delta^{18}\text{O}$ and
356 $\Delta^{17}\text{O}$ values enriched in both ^{18}O and ^{17}O , more than +55 ‰ and more than +18 ‰,
357 respectively, during summer periods in Japan (Tsunogai et al., 2016), the nitrate-
358 enriched endmember showed the $\delta^{18}\text{O}$ and $\Delta^{17}\text{O}$ values depleted in both ^{18}O and ^{17}O ,
359 less than +3.1 ‰ and +1.6 ‰, respectively, during the storm events. During storm
360 events, increase in $\delta^{18}\text{O}$ and/or $\Delta^{17}\text{O}$ have been reported for stream nitrate eluted from
361 forested catchments in past studies (Sebestyén et al., 2019; Sabo et al., 2016; Buda
362 and Dewalle. 2009). In KJ catchment, however, we found significant decrease in both
363 the $\delta^{18}\text{O}$ and $\Delta^{17}\text{O}$ of stream nitrate during storm events. In addition, tThe
364 concentrations of $\text{NO}_3^-_{\text{atm}}$ ($[\text{NO}_3^-_{\text{atm}}]$) showed little temporal variations showing the
365 concentrations of $1.6 \pm 0.4 \mu\text{M}$, $1.8 \pm 0.4 \mu\text{M}$, and $2.1 \pm 0.4 \mu\text{M}$ during the storm
366 events I, II, and III, respectively (Figs. 3e, S1e, and S1j). In general, the $[\text{NO}_3^-_{\text{atm}}]$ in
367 rainwater were much higher than those in stream water (Nakagawa et al., 2018; Rose
368 et al., 2015; Tsunogai et al., 2014). During the storm events I, II, and III, however, the
369 $[\text{NO}_3^-_{\text{atm}}]$ in stream water was almost constant irrespective to the increase in
370 precipitation (Figs. 3e, S1e, and S1j).—Thus, we conclude that the direct input of
371 $[\text{NO}_3^-_{\text{atm}}]$ via rainwater into the stream through overland flow during storm events can
372 be negligible, at least in the KJ catchment. Thus, we concluded that the $\text{NO}_3^-_{\text{atm}}$
373 should be the minor source of nitrate that increased during the storm events.

374 Nakagawa et al. (2018) determined the temporal variations in the concentrations
375 (Fig. 5a) and isotopic compositions ($\delta^{15}\text{N}$, $\delta^{18}\text{O}$, and $\Delta^{17}\text{O}$) (Figs. 5b, 5c, and 5d) of
376 soil nitrate dissolved in soil water taken within the same catchment during 2013 to
377 2014, at the depths of 20 cm and 60 cm of the station SLS (SLS 20 and SLS 60,
378 respectively) and at the depth of 20 cm of the station SMS (SMS 20), where the
379 station SLS was located in the riparian zone of the stream and the station SMS was
380 about 20 m away from the stream and located in the upland zone (Fig. 1b). The
381 concentrations of soil nitrate showed significant seasonal variation, with the higher
382 concentration in summer and the lower concentration in winter (Fig. 5a). Both the
383 $\delta^{18}\text{O}$ and $\Delta^{17}\text{O}$ values also showed significant seasonal variation, with the minimum
384 in summer and the maximum in winter (Figs. 5c and d). To verify if the soil nitrate is
385 the source of the stream nitrate that was added to the stream during the storm events,
386 we also plotted soil nitrate at each site (SLS 20, SLS 60 and SMS 20) of the same
387 season in Fig. 4. Because our intensive observations on the storm events were done in
388 summer (from August to October), the average concentration and the average isotopic
389 composition during summer (from August to October) were calculated (Table 2+) and
390 plotted in Fig. 4. The error bars of each soil nitrate denote the standard deviation (SD)
391 of each isotopic composition ($n=5$ for each). We found that the isotopic compositions
392 ($\delta^{15}\text{N}$, $\delta^{18}\text{O}$, and $\Delta^{17}\text{O}$) of soil nitrate in the riparian zone (SLS 20 and SLS 60; Table
393 2+) were always plotted on the nitrate-enriched extension (lower $1/[\text{NO}_3^-]$ extension)
394 of the mixing line during the storm events I, II, and III (Fig. 4), while those of the soil

395 nitrate in the upland zone (SMS 20; Table 2+) were somewhat deviated from the
396 nitrate-enriched extension of the mixing line, $\delta^{18}\text{O}$ especially (Figs. 4d, 4e, and 4f).
397 We conclude that the primary source of nitrate added during the storm events was the
398 soil nitrate in the riparian zone.

399 The “flushing hypothesis” has been proposed to explain the increase in stream
400 nitrate concentration in accordance with the increase in flow rate during storm events
401 (Creed et al., 1996; Hornberger et al., 1994). During the base flow periods, nitrate
402 accumulate in shallow, oxic soil layers due to the progress of nitrification. When
403 water level became higher during storm periods, concentration of stream nitrate
404 increased due to flushing of the soil nitrate accumulated in the shallow soil layers of
405 riparian zones into stream (Chen et al., 2020; Creed et al., 1996; Ocampo et al., 2006).
406 Our finding that the primary source of nitrate increased during the storm events was
407 the soil nitrate in the riparian zone is consistent with the “flushing hypothesis.” We
408 conclude that the flushing of soil nitrate in the riparian zone into the stream due to
409 rising of both stream water and groundwater level was primarily responsible for the
410 increase in stream nitrate during the storm events (Fig. 6).–

411 Within the whole dataset on the variation of the concentration of nitrate in the stream
412 determined by Kamisako et al. (2008), ~~an~~ increases in the concentration of stream
413 nitrate ~~in the stream of~~ to more than 20 μM in response to storm events ~~was found to~~
414 ~~be~~ were limited to the storm events that occurred in the warm ~~seasons~~ months, from June
415 to November. As the concentrations of soil nitrate in the riparian zone (SLS 20 and SLS

416 60) were much higher in the warm ~~seasons~~ months ($734 \mu\text{M} \pm 496 \mu\text{M}$; from June to
417 November) than in the cold ~~seasons~~ months ($156 \pm 124 \mu\text{M}$; from December to May),
418 such seasonal variation in the concentration of riparian soil nitrate is consistent with the
419 observed seasonality in the influence of storm events on the stream nitrate concentration,
420 where significant ~~effects~~ increase ~~are observed during~~ were limited to warm months,
421 whereas insignificant effects are observed during cold months.

422 The stream nitrate during storm events showed $\delta^{15}\text{N}$ values more depleted in ^{15}N than
423 those during the base flow periods (Figs. 3b, S1b, and S1g), probably due to the input
424 of riparian soil nitrate more depleted in ^{15}N . Compared with the $\delta^{15}\text{N}$ values of stream
425 nitrate taken during the base flow periods of routine observations when precipitation
426 was less than 1 mm/day (Fig. 2b; Table S1), the riparian soil nitrate (SLS 20 and SLS
427 60; Table 2) showed the $\delta^{15}\text{N}$ values around 3.5 ‰ lower. The trend and the extent of
428 the ^{15}N -depletion coincided well with those determined in the forested catchments in
429 past studies (Fang et al., 2015; Hattori et al., 2019). Fang et al. (2015), for instance,
430 reported significant differences between the $\delta^{15}\text{N}$ values of soil nitrate and those of
431 stream nitrate in six forested catchments in Japan and China, and proposed that the
432 kinetic fractionation due to the progress of denitrification during the elution of soil
433 nitrate into groundwater was responsible for the relative ^{15}N -enrichment in stream
434 nitrate compared with soil nitrate. As a result, the observed temporal decrease in the
435 $\delta^{15}\text{N}$ value of stream nitrate during storm events also supported that the flushing of soil
436 nitrate showing ^{15}N -depleted $\delta^{15}\text{N}$ values into the stream was responsible for the

437 elevated of nitrate concentrations during storm events.

438 As mentioned in section 3.1, we found significant increase in nitrate concentration
439 up to 129.3 μM on 2018/8/31 during our routine observation on the stream, when the
440 water was sampled in the middle of a heavy storm (~~59.5~~48.0 mm/~~per~~ day; Table S1)
441 with significant increase in flow rate (from 53.4 L/min one month before to 216.9
442 L/min during sampling), which the amount of precipitation on 2018/8/31 was the
443 highest within the whole routine observations (Table S1). The measured $\delta^{18}\text{O}$ and
444 $\Delta^{17}\text{O}$ value of the stream nitrate on 2018/8/31 (-1.9‰ and $+0.4\text{‰}$, respectively),
445 showing significantly smaller values than those during the other routine observation
446 (Fig. 2c and 2d), agreed well with those of the nitrate increase during the storm events
447 I, II, and III. Moreover, both the range of increase in stream nitrate concentration
448 (129.3 μM) and the season of observation (August) also agreed well with those of the
449 stream nitrate increase during the three storm events. As a result, we conclude that the
450 input of soil nitrate accumulated in the riparian zone due to flushing was also
451 responsible for the significant increase in stream nitrate concentration we found on
452 2018/8/31 during the routine observation.

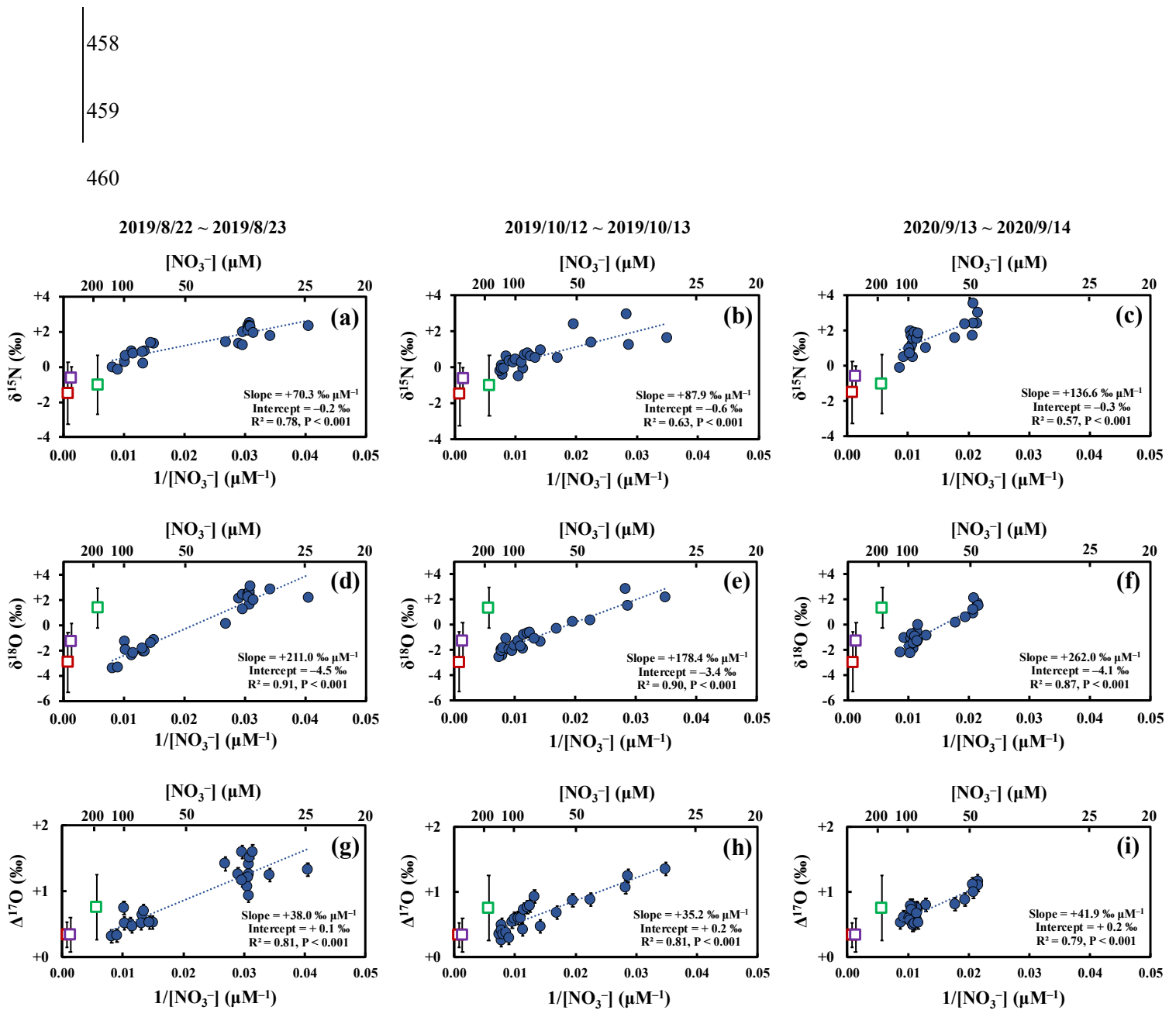
453

454

455

456

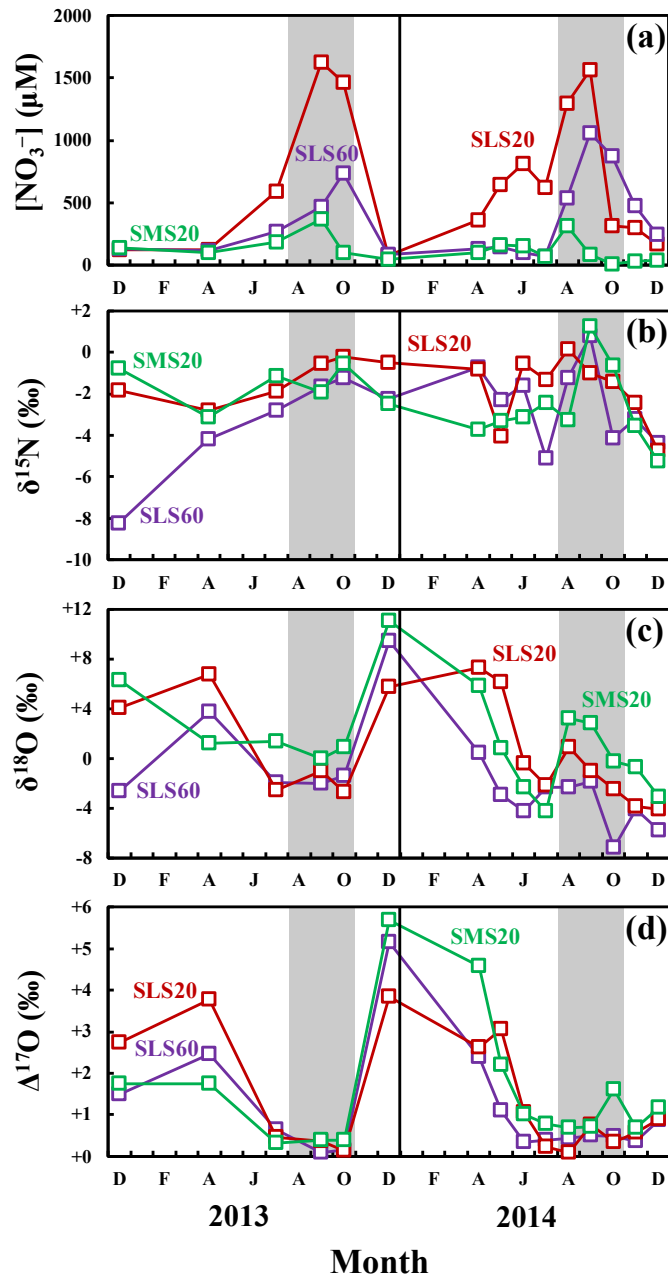
457



461 **Figure 4.** The $\delta^{15}\text{N}$ (a, b, and c), $\delta^{18}\text{O}$ (d, e, and f), and $\Delta^{17}\text{O}$ (g, h, and i) values of
 462 stream nitrate (blue circles) during storm events I, II, and III plotted as a function of the
 463 reciprocal of nitrate concentration ($1/[\text{NO}_3^-]$), together with those of soil nitrate at SLS
 464 20 (red squares; riparian zone), SLS 60 (purple squares; riparian zone), and SMS 20
 465 (green squares; upland zone) during August to October in 2013 and 2014. The error
 466 bars of each soil nitrate denote the standard deviation (SD) of each isotopic composition

467 (n =5 for each). The error bars smaller than the sizes of the symbols are not presented.

468

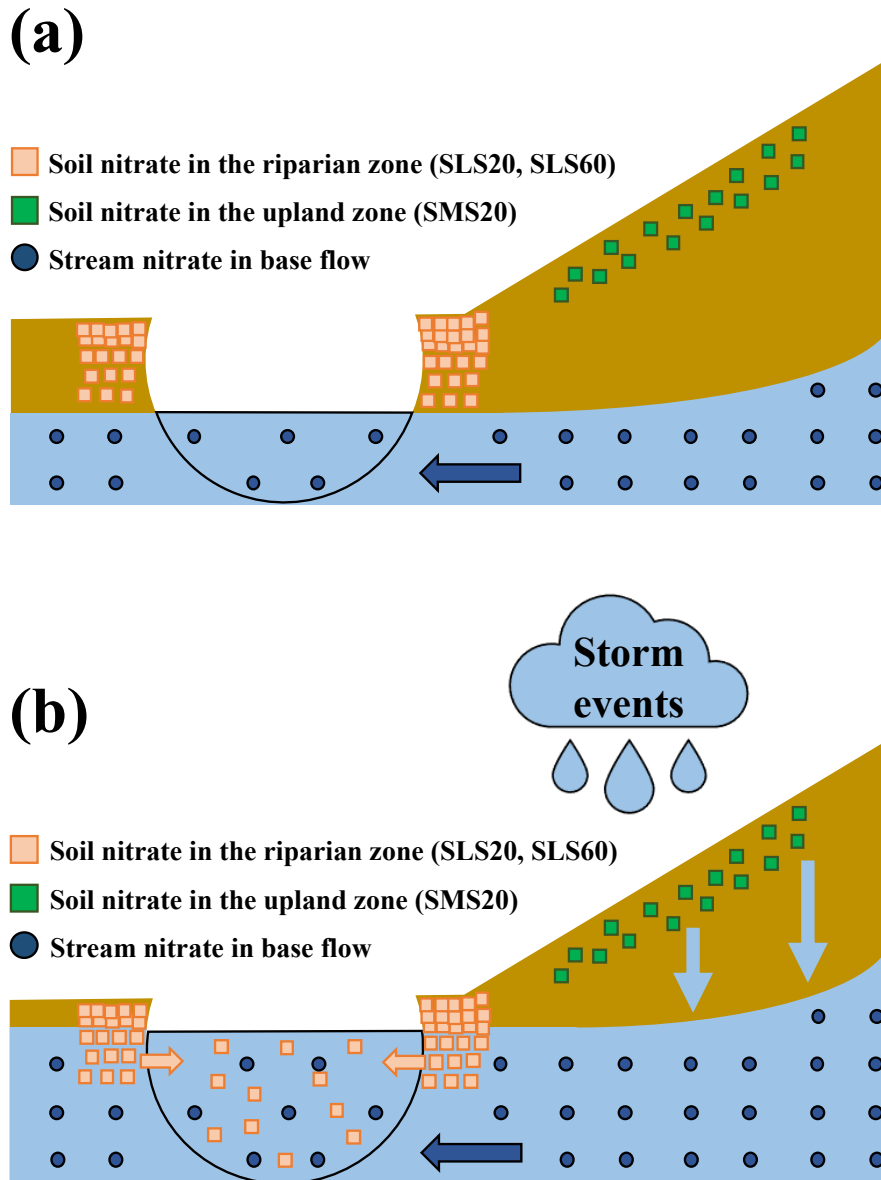


469 **Figure 5.** Seasonal variations in the concentrations of soil nitrate (a) at SLS 20 (red
470 squares), SLS 60 (purple squares), and SMS20 (green squares), together with those in
471 the values of $\delta^{15}N$ (b), $\delta^{18}O$ (c) and $\Delta^{17}O$ (d) of each soil nitrate during 2013 to 2014
472 (modified from Nakagawa et al., 2018). The periods used to estimate the isotopic

473 compositions (from August to October) are presented in gray. The error bars were
 474 smaller than the sizes of the symbols.

475 **Table 2+.** Concentrations and isotopic compositions ($\delta^{15}\text{N}$, $\delta^{18}\text{O}$, and $\Delta^{17}\text{O}$) of soil
 476 nitrate at SLS 20, SLS 60, and SMS 20 during August to October in 2013 and 2014
 477 (recalculated from the data in Nakagawa et al., 2018).

	SLS 20	SLS 60	SMS 20
478 NO_3^- (μM)	1254 \pm 537	734 \pm 241	176 \pm 159
479 1000 $\delta^{15}\text{N}$	-1.5 \pm 1.8	-0.6 \pm 0.6	-1.0 \pm 1.7
480 1000 $\delta^{18}\text{O}$	-2.9 \pm 2.4	-1.3 \pm 1.4	+1.4 \pm 1.6
1000 $\Delta^{17}\text{O}$	+0.3 \pm 0.2	+0.3 \pm 0.3	+0.8 \pm 0.5



482 **Figure 6.** Schematic diagram showing the elution of soil nitrate to the stream before
 483 the storm events (a) and during the storm events (b). Soil nitrate in the riparian zone
 484 and that in the upland zone are represented by the orange squares and green squares,
 485 respectively, while stream nitrate during base flow is represented by the blue circles.

486

487 4.3.2 Variation in the concentration of $\text{NO}_3^-_{\text{atm}}$ during routine observation

488 The concentration of $\text{NO}_3^-_{\text{atm}}$ ($[\text{NO}_3^-_{\text{atm}}]$) showed little seasonal variation, from 1.3
489 μM to 3.8 μM during our routine observation in this study (Fig. 2e), except for the
490 extraordinarily large $[\text{NO}_3^-_{\text{atm}}]$ we found on 2019/1/31 (6.5 μM). Except for the
491 extraordinarily large $[\text{NO}_3^-_{\text{atm}}]$, the obtained $[\text{NO}_3^-_{\text{atm}}]$ corresponded well with those
492 determined in the past study done at the same catchment (Nakagawa et al., 2018). In
493 addition, they corresponded well with those of the temperate forested catchments
494 saturated in nitrogen, such as [Qingyuan Forest \(2.0 \$\mu\text{M}\$; Huang et al., 2020\)](#) and Fernow
495 experimental Forest [1, 2, and 3 \(1.6 \$\mu\text{M}\$, 3.4 \$\mu\text{M}\$, and 4.2 \$\mu\text{M}\$, respectively; Rose et al.,](#)
496 2015).

497 In this study, accumulation of snow up to 18 cm was observed at the KJ catchment
498 on 2019/1/27, ~~of up to 18 cm,~~ while most of the accumulated snow had melted to a
499 depth of 1 cm ~~depth~~ by 2019/1/30, ~~prior to~~ just before the sampling ~~being carried out~~ on
500 2019/1/31. Furthermore, during the routine observation period from 2017/5 to 2020/3,
501 no other snow-melting events ~~were experienced~~ occurred within 4 days prior to the day
502 of sampling ~~day~~, except for the sampling on 2019/1/31. Similar enhancement in the
503 concentration of $\text{NO}_3^-_{\text{atm}}$, as well as the $\delta^{18}\text{O}$ and $\Delta^{17}\text{O}$ of stream nitrate, in response to
504 snow melting has been frequently observed in streams worldwide (Ohte et al., 2004,
505 2010; Pellerin et al., 2012; Piatek et al., 2005; Rose et al., 2015; Sabo et al., 2016;
506 Tsunogai et al., 2014, 2016).

507 The flow rate, concentration of stream nitrate, and $\Delta^{17}\text{O}$ was 110.0 L/min, 70.0 μM ,
508 and +1.17 ‰ on 2018/12/28, respectively, while 117.3 L/min, 62.4 μM , and +2.73 ‰

509 on 2019/1/31, respectively (Table S1). The $[\text{NO}_3^-]_{\text{atm}}$ in stream water was estimated to
510 be 3.1 μM on 2018/12/28 and 6.5 μM on 2019/1/31. Assuming that the $[\text{NO}_3^-]_{\text{atm}}$ in
511 snow melt was the same with the volume-weighted mean concentration of nitrate in
512 rainwater (41.0 μM) determined at Sado island in January (EANET, 2010, 2011;
513 Tsunogai et al., 2016), the increase in the flow rate ($\Delta F_{\text{snowmelt}}$) due to the mixing of
514 snow melt into the stream can be estimated to be 10.3 L/min, by using the mass balance
515 equation shown below:

$$516 \quad ([\text{NO}_3^-]_{\text{atm}})_{2019/1/31} \times F_{2019/1/31} = [\text{NO}_3^-]_{\text{atm}})_{2018/12/28} \times F_{2018/12/28} + [\text{NO}_3^-]_{\text{atm}})_{\text{snowmelt}} \times$$
$$517 \quad \Delta F_{\text{snowmelt}} \quad (3)$$

518 where $[\text{NO}_3^-]_{\text{atm}})_{2018/12/28}$, $[\text{NO}_3^-]_{\text{atm}})_{2019/1/31}$, and $[\text{NO}_3^-]_{\text{atm}})_{\text{snowmelt}}$ denote the $[\text{NO}_3^-]_{\text{atm}}$ in
519 stream water on 2018/12/28, 2019/1/31, and that in snow melt water, respectively, and
520 $F_{2018/12/28}$, $F_{2019/1/31}$, and $\Delta F_{\text{snowmelt}}$ denote the flow rate of stream water on 2018/12/28,
521 2019/1/31, and the increase in the flow rate due to snow melt, respectively. Because the
522 estimated volume of melting snow water into the stream water (10.3 L/min) was
523 comparable with the observed increase in the flow rate from 2018/12/28 to 2019/1/31
524 (7.3 L/min), we concluded that the snow melting was responsible for the increase in
525 $\Delta^{17}\text{O}$ on 2019/1/31 and ~~We conclude~~ that ~~the~~ input of ~~the~~ NO_3^- accumulated in the

526 melted snow water, showing $\delta^{18}\text{O}$ and $\Delta^{17}\text{O}$ values significantly higher than those in
527 the stream, caused the extraordinarily increase in $[\text{NO}_3^-]_{\text{atm}}$ on 2019/1/31. Except for
528 the extraordinarily increase in $[\text{NO}_3^-]_{\text{atm}}$ ($n = 1$), $[\text{NO}_3^-]_{\text{atm}}$ was stable at $2.2 \pm 0.6 \mu\text{M}$
529 throughout the routine observation ($n = 33$). We concluded that $[\text{NO}_3^-]_{\text{atm}}$ was generally

530 stable in the stream.

531

532 4.4.3 The impact of storm events on the index of the nitrogen saturation

533 The concentration of stream nitrate eluted from a forested catchment has been used

534 as an index to evaluate the stage of nitrogen saturation ~~in the forest~~ (Huang et al., 2020;

535 Rose et al., 2015; Stoddard, 1994). However, McHale et al. (2002) pointed out the

536 problem in the reliability of this index, because the number of storm events influenced

537 the concentration of nitrate eluted from forested stream significantly. That is, if we use

538 the concentration of stream nitrate sampled during the storm events to evaluate the stage

539 of nitrogen saturation in a forested catchment, the stage of nitrogen saturation might be

540 overestimated.

541 Nakagawa et al. (2018) have proposed the export flux of $\text{NO}_3^-_{\text{atm}}$ (M_{atm}) relative to

542 the deposition flux of $\text{NO}_3^-_{\text{atm}}$ (D_{atm}) can be an alternative, more robust index for

543 nitrogen saturation in temperate forested catchments, because the $M_{\text{atm}}/D_{\text{atm}}$ ratio

544 directly reflect the demand on atmospheric nitrate deposited onto each forested

545 catchments as a whole, and thus reflect the nitrogen saturation in each forested

546 catchment. To estimate reliable M_{atm} in each forested catchment, we must obtain

547 reliable $[\text{NO}_3^-_{\text{atm}}]$ in the forested stream, including their temporal variation. ~~While the~~

548 ~~past studies focused on the seasonal variation of concentration and export flux of~~

549 ~~$\text{NO}_3^-_{\text{atm}}$ in forested streams (Hattori et al., 2019; Nakagawa et al., 2018; Rose et al.,~~

550 ~~2015; Sabo et al., 2016; Tsunogai et al., 2014), we had little knowledge on the variation~~

551 ~~of $[\text{NO}_3^-]_{\text{atm}}$ in response to the increase in nitrate concentration during storm events~~
552 ~~prior to this study.~~

553 As already presented in section 4.2~~1~~, we found that $[\text{NO}_3^-]_{\text{atm}}$ remained almost
554 constant irrespective to the significant variation in $[\text{NO}_3^-]$ during storm events (Figs.
555 3e, S1e, and S1j). The concentrations of atmospheric nitrate ($[\text{NO}_3^-]_{\text{atm}}$) in rainwater
556 were much higher than those in stream water. While the volume-weighted mean
557 $[\text{NO}_3^-]_{\text{atm}}$ in rainwater determined in Sado island from August to October, for example,
558 was $15.2 \pm 8.4 \mu\text{M}$ (EANET, 2010, 2011; Tsunogai et al., 2016), that in the stream water
559 was $2.2 \pm 0.6 \mu\text{M}$ in this study. As a result, the $[\text{NO}_3^-]_{\text{atm}}$ in stream water would increase,
560 if significant portion of rainwater was added directly into the stream water during the
561 storm events. The $[\text{NO}_3^-]_{\text{atm}}$ in stream water, however, was stable showing no
562 correlation with the amount of precipitation or the concentration of stream nitrate during
563 the storm events (Figs. 3e, S1e, and S1j). The $[\text{NO}_3^-]_{\text{atm}}$ remained almost constant as
564 well during the stream event on 2018/8/31 we found through the routine observation,
565 while $[\text{NO}_3^-]$ increased from $35.7 \mu\text{M}$ (1 month before) to $129.3 \mu\text{M}$ (Fig. 2e). As a
566 result, we concluded that the direct input of NO_3^- into the stream water was negligible
567 even during the storm events. ~~Furthermore, during our routine observation on~~
568 ~~2018/8/31, the $[\text{NO}_3^-]_{\text{atm}}$ remained almost constant as well, while $[\text{NO}_3^-]$ increased~~
569 ~~from $35.7 \mu\text{M}$ (1 month before) to $129.3 \mu\text{M}$ (Fig. 2e).~~

570 The observed $[\text{NO}_3^-]_{\text{atm}}$ showing almost constant values implies that the primary
571 source of NO_3^- in stream water during storm events was the NO_3^- stored in

572 groundwater, which is the same source as that during the base flow periods, rather than
573 the direct input of NO_3^- from rainwater ~~through overland flow~~. Because direct input
574 of NO_3^- into stream water was negligible during the storm events, the $M_{\text{atm}}/D_{\text{atm}}$ ratio
575 in each forested catchment should be controlled by Hence, ~~on the basis of the data of~~
576 ~~the annual average flow rate of the stream from the catchment, a reliable annual M_{atm}~~
577 ~~can be estimated from $[\text{NO}_3^-]_{\text{atm}}$, even if the $[\text{NO}_3^-]_{\text{atm}}$ data during storm events is~~
578 ~~included. While the annual M_{atm} could increase in response to the increase in the number~~
579 ~~of storm events because of the increase in the flow rate, the annual D_{atm} also increases~~
580 ~~in response to the increase in the number of storm events. Consequently, it can be~~
581 ~~concluded that storm events have little impact on the $M_{\text{atm}}/D_{\text{atm}}$. As long as NO_3^-~~
582 ~~experiences~~ the metabolized processes (uptake or denitrification) in each forested
583 catchment subsequent to deposition, so that the $M_{\text{atm}}/D_{\text{atm}}$ can correctly reflect the total
584 demand on NO_3^- in each forested catchment and thus the status of nitrogen saturation
585 status. We conclude that the $M_{\text{atm}}/D_{\text{atm}}$ ratio can be ~~used as the~~ a more robust index to
586 evaluate nitrogen saturation in forested catchments, ~~on which storm events have little~~
587 influence.

588

589 **5 Conclusions**

590 Temporal variations in the concentrations and stable isotopic compositions ($\delta^{15}\text{N}$,
591 $\delta^{18}\text{O}$, and $\Delta^{17}\text{O}$) of stream nitrate were determined during storm events to clarify the
592 source of stream nitrate increased during storm events. Because the stable isotopic

593 compositions of soil nitrate in riparian zone during summer agreed well with those of
594 the nitrate-enrich endmember of the stream nitrate increased during storm events, we
595 conclude that the soil nitrate in riparian zone was primarily responsible for the stream
596 nitrate increase during storm events. Additionally, the concentration of $\text{NO}_3^-_{\text{atm}}$ in the
597 stream was almost constant during the storm events, implied that the source of $\text{NO}_3^-_{\text{atm}}$
598 in stream water during storm events was the $\text{NO}_3^-_{\text{atm}}$ stored in groundwater. We
599 concluded that the number of storm events have little impact on $M_{\text{atm}}/D_{\text{atm}}$ ratio, the
600 index of nitrogen saturation. In addition, the $\Delta^{17}\text{O}$ of nitrate can be applicable as the
601 tracer to clarify the source of nitrate.

602

603

604

605

606

607

608

609

610

611

612

613

614 Appendix A: Possible alterations to the concentration and isotopic compositions of
615 stream nitrate during the storage period in the automatic sampler used for the
616 intensive observations

617 During the intensive observations, the stream water samples were stored in bottles of
618 the automatic sampler. The storage periods until filtration were ranged from 7 (storm
619 event I) to 12 days (storm event III) (Table 1). While the automatic sampler was
620 surrounded by ferns and the other understory vegetations to minimize the possible
621 alterations on the samples, progress of biogeochemical reactions such as nitrification,
622 denitrification, and assimilation could alter the concentration and isotopic compositions
623 ($\delta^{15}\text{N}$, $\delta^{18}\text{O}$, and $\Delta^{17}\text{O}$) of stream nitrate during the storage period. Above all, possible
624 increase in soil water input into the stream water that is enriched with organic matters
625 during a storm event could enhance nitrification during the storage period and could
626 increase the concentration of nitrate in the stream water samples taken by using the
627 automatic sampler. Here, we discussed the possible alteration of the concentration and
628 isotopic compositions during the storage for the samples taken by using the automatic
629 sampler.

630 First, we compared the samples taken during the intensive observations using the
631 automatic sampler with those taken during the routine observations. During the routine
632 observations, the stream water samples were taken manually, transported to the
633 laboratory within 1 h of each collection, passed through a membrane filter (pore size
634 0.45 μm), and stored in a refrigerator (4°C) until chemical analysis. As a result,

635 alterations should be minor in the samples taken through the routine observations.

636 When we compared the concentrations and isotopic compositions of stream nitrate
637 in the samples taken at the beginning of the intensive observation using the automatic
638 sampler with those in the routine observation nearby, they coincided well each other
639 (Table A1), implying that at least the progress of nitrification within the bottles of the
640 automatic sampler should be minor during the storage period because the concentration
641 of nitrate should increase, while the $\Delta^{17}\text{O}$ should decreased significantly during the
642 storage period if the progress of nitrification was active in the bottles of the intensive
643 observation.

644 In addition, a clear storm event was also observed during the routine observation on
645 2018/8/31 (Fig. 2; Table S1), so that we can compare the concentrations and isotopic
646 compositions of stream nitrate with those of intensive observations. During the routine
647 observation on 2018/8/31 done under a precipitation and flow rate of 48 mm/day and
648 216.9 L/min, respectively, we observed a significant increase in the concentration of
649 stream nitrate from 35.7 μM one month before to 129.3 μM (Fig. 2 and Table S1). In
650 accordance with the increase in the concentration, we found significant changes in the
651 isotopic compositions; from +5.9 ‰ to +1.8 ‰ for $\delta^{15}\text{N}$, from +4.1 ‰ to -1.9 ‰ for
652 $\delta^{18}\text{O}$, from +1.5 ‰ to +0.4 ‰ for $\Delta^{17}\text{O}$ (Fig. 2 and Table S1). The trend and the degree
653 of the variations in the concentration and the isotopic compositions on 2018/8/31 from
654 those on one month before were consistent with those of the intensive observation (Figs.
655 3 and S1). As a result, we concluded that the increase in the flow rate was responsible

656 for the observed increase in concentrations of stream nitrate during the storm events
657 and thus the microbial production of nitrate through nitrification during the storage had
658 little influence on the observed temporal changes in the concentrations and isotopic
659 compositions of nitrate in the stream water samples taken by using the automatic
660 sampler.

661 Kotlash and Chessman (1998) conducted storage experiments under various
662 conditions such as freezing, acidification, refrigeration, and room temperature to clarify
663 the changes in the concentrations of nitrogen compounds in stream water samples and
664 found little change in concentration of oxidized nitrogen ($\text{NO}_3^- + \text{NO}_2^-$) irrespective of
665 the treatments. To further verify the insignificant changes in the concentrations and
666 isotopic compositions of stream nitrate stored without treatments in the samples taken
667 by the automatic sampler, we also conducted the storage experiments by using a 100
668 mL of stream water taken at the KJ forested catchment on 2022/4/28 and stored in a
669 100 ml PP (polypropylene) bottle without treatments. Approximately 85 mL of the
670 stream water within the bottle was filtered using a GF/F filter paper (25 mm diameter)
671 and stored in a refrigerator (4°C) to determine original (initial) concentration and
672 isotopic compositions of nitrate. To simulate the stream water containing increased
673 suspended organic matters during the storm events, the GF/F filter paper was returned
674 to the 100 mL PP bottle which contained 15 mL of the stream water sample and left the
675 15 mL stream water under the room temperature (18.3°C) for 2 weeks together with the
676 suspended organic matters on the filter. The concentration and isotopic compositions of

677 the original stream nitrate (85 mL) and those being stored without filtration under the
678 room temperature for 2 weeks (15 mL) were analyzed by using the same method
679 presented in section 2.4. The concentration of nitrate in the stream water sample being
680 stored for 2 weeks without treatments coincided well with those in the original, showing
681 the difference in concentrations less than 10 % (Table A2). Besides, the differences in
682 the isotopic compositions from the original were also negligibly small (Table A2).

683 As a result, we concluded that the possible alteration in the concentration and isotopic
684 compositions of nitrate due to the progress of biogeochemical reactions such as
685 nitrification, denitrification, and assimilation during storage in the automatic sampler
686 used in the intensive observations was negligibly small.

687
688
689
690
691
692
693
694
695
696
697

698 Table A1. Comparison of both concentration and isotopic compositions ($\delta^{15}\text{N}$, $\delta^{18}\text{O}$,
 699 and $\Delta^{17}\text{O}$) of stream nitrate between those taken at the beginning of intensive
 700 observations using the automatic sampler and those taken manually on the days nearby
 701 during routine observations.

	<u>Type</u>	<u>Flow rate</u> <u>L/min</u>	<u>Precipitation</u> <u>mm/day</u>	<u>NO₃⁻</u> <u>μM</u>	<u>δ¹⁵N</u> <u>/10³</u>	<u>δ¹⁸O</u> <u>/10³</u>	<u>Δ¹⁷O</u> <u>/10³</u>
<u>2019/7/31</u>	<u>routine</u>	<u>61.6</u>	<u>0.0</u>	<u>39.5</u>	<u>+1.55</u>	<u>+0.66</u>	<u>+1.06</u>
<u>2019/8/22 16:00</u>	<u>intensive</u>	<u>64.1</u>	<u>1.0</u>	<u>24.7</u>	<u>+2.32</u>	<u>+2.17</u>	<u>+1.33</u>
<u>2019/8/30</u>	<u>routine</u>	<u>66.0</u>	<u>13.0</u>	<u>44.9</u>	<u>+2.07</u>	<u>-0.13</u>	<u>+0.91</u>
<u>2019/9/30</u>	<u>routine</u>	<u>28.0</u>	<u>0.0</u>	<u>37.9</u>	<u>+1.65</u>	<u>+1.56</u>	<u>+1.36</u>
<u>2019/10/12 15:00</u>	<u>intensive</u>	<u>22.4</u>	<u>7.0</u>	<u>28.7</u>	<u>+1.61</u>	<u>+2.18</u>	<u>+1.35</u>
<u>2019/10/31</u>	<u>routine</u>	<u>32.6</u>	<u>0.0</u>	<u>50.4</u>	<u>+1.04</u>	<u>+0.19</u>	<u>+0.92</u>
<u>2020/9/13 11:00</u>	<u>intensive</u>	<u>111.0</u>	<u>0.0</u>	<u>46.6</u>	<u>+2.42</u>	<u>+1.74</u>	<u>+1.17</u>
<u>2020/9/30</u>	<u>routine</u>	<u>117.3</u>	<u>0.0</u>	<u>63.2</u>	<u>=</u>	<u>=</u>	<u>=</u>

702 –:No samples were taken for isotopic analysis

703

704 Table A2. Comparison of both concentration and isotopic compositions ($\delta^{15}\text{N}$, $\delta^{18}\text{O}$,
 705 and $\Delta^{17}\text{O}$) between original stream water sample and that being stored under the room
 706 temperature for 2 weeks without treatments.

	<u>NO₃⁻</u> <u>μM</u>	<u>δ¹⁵N</u> <u>/10³</u>	<u>δ¹⁸O</u> <u>/10³</u>	<u>Δ¹⁷O</u> <u>/10³</u>
<u>Original</u>	<u>53.2</u>	<u>+0.90</u>	<u>+0.80</u>	<u>+1.05</u>
<u>Stored</u>	<u>49.5</u>	<u>+0.85</u>	<u>+0.90</u>	<u>+0.99</u>

707

708 *Data availability.* All the primary data are presented in the Supplement. The other data
 709 are available upon request to the corresponding author (Weitian Ding).

710

711 *Author contributions.* WD, UT, NY, and HS designed the study. HY, MM, and HS
712 performed the field observations. HY, MM, and HS determined the concentrations of
713 the samples. WD determined the isotopic compositions of the samples. WD, TS, FN,
714 and UT performed data analysis, and WD and UT wrote the paper with input from MM,
715 HY and HS.

716

717 *Competing interests.* The authors declare that they have no conflict of interest.

718

719 *Acknowledgements.*

720 We thank anonymous referees for valuable remarks on an earlier version of this
721 paper. The samples analyzed in this study were collected through the Long-term
722 Monitoring of Transboundary Air Pollution and Acid Deposition by the Ministry of
723 the Environment in Japan. The authors are grateful to Ryo Shingubara, Masanori Ito,
724 Hao Xu, Hui Lan, Peng Lai, Tianzheng Huang, Yuhei Morishita, Tae Ito, Yuka
725 Tadachi and other present and past members of the Biogeochemistry Group, Nagoya
726 University, for their valuable support throughout this study. This work was supported
727 by a Grant-in-Aid for Scientific Research from the Ministry of Education, Culture,
728 Sports, Science, ~~and~~ Technology of Japan under grant numbers JP17H00780,
729 JP19H04254, and JP19H00955 ~~and~~ ~~by~~ the Yanmar Environmental Sustainability
730 Support Association, and the River Fund of The River Foundation, Japan. Weitian

731 [Ding would like to take this opportunity to thank the ‘Nagoya University](#)
732 [Interdisciplinary Frontier Fellowship’ supported by JST and Nagoya University.](#)

733

734 **Reference**

735 Aber, J. D., Nadelhoffer, K. J., Steudler, P. and Melillo, J. M.: Nitrogen Saturation in
736 Northern Forest Ecosystems, *Bioscience*, 39(6), 378–386, doi:10.2307/1311067,
737 1989.

738 Aguilera, R. and Melack, J. M.: Concentration-Discharge Responses to Storm Events
739 in Coastal California Watersheds, *Water Resour. Res.*, 54(1), 407–424,
740 doi:10.1002/2017WR021578, 2018.

741 Alexander, B., Hastings, M. G., Allman, D. J., Dachs, J., Thornton, J. A. and
742 Kunasek, S. A.: Quantifying atmospheric nitrate formation pathways based on a
743 global model of the oxygen isotopic composition ($\delta^{17}\text{O}$) of atmospheric nitrate,
744 *Atmos. Chem. Phys.*, 9(14), 5043–5056, doi:10.5194/acp-9-5043-2009, 2009.

745 [Buda, A. R. and DeWalle, D. R.: Dynamics of stream nitrate sources and flow](#)
746 [pathways during stormflows on urban, forest and agricultural watersheds in central](#)
747 [Pennsylvania, USA, *Hydrol. Process.*, 23\(23\), 3292–3305,](#)
748 [doi:https://doi.org/10.1002/hyp.7423, 2009.](#)

749 Burns, D. A. and Kendall, C.: Analysis of $\delta^{15}\text{N}$ and $\delta^{18}\text{O}$ to differentiate NO_3^- sources
750 in runoff at two watersheds in the Catskill Mountains of New York, *Water Resour.*
751 *Res.*, 38(5), 91–912, doi:10.1029/2001wr000292, 2002.

752 [Burns, D. A., Pellerin, B. A., Miller, M. P., Capel, P. D., Tesoriero, A. J. and Duncan,](#)
753 [J. M.: Monitoring the riverine pulse: Applying high-frequency nitrate data to advance](#)
754 [integrative understanding of biogeochemical and hydrological processes, Wiley](#)
755 [Interdiscip. Rev. Water, \(October 2018\), e1348, doi:10.1002/wat2.1348, 2019.](#)

756 Chen, X., Tague, C. L., Melack, J. M. and Keller, A. A.: Sensitivity of nitrate
757 concentration-discharge patterns to soil nitrate distribution and drainage properties in
758 the vertical dimension, *Hydrol. Process.*, 34(11), 2477–2493, doi:10.1002/hyp.13742,
759 2020.

760 [Christopher, S. F., Mitchell, M. J., McHale, M. R., Boyer, E. W., Burns, D. A. and](#)
761 [Kendall, C.: Factors controlling nitrogen release from two forested catchments with](#)
762 [contrasting hydrochemical responses, *Hydrol. Process.*, 22\(1\), 46–62,](#)
763 [doi:https://doi.org/10.1002/hyp.6632, 2008.](#)

764 Creed, I. F., Band, L. E., Foster, N. W., Morrison, I. K., Nicolson, J. A., Semkin, R. S.
765 and Jeffries, D. S.: Regulation of nitrate-N release from temperate forests: A test of
766 the N flushing hypothesis, *Water Resour. Res.*, 32(11), 3337–3354,
767 doi:10.1029/96WR02399, 1996.

768 Durka, W., Schulze, E., Gebauer, G. and Voerkeliust, S.: Effects of forest decline on
769 uptake and leaching of deposited nitrate determined from ¹⁵N and ¹⁸O measurements,
770 *Nature*, 372, 765–767, doi: https://doi.org/10.1038/372765a0, 1994.

771 [EANET: Data Report 2010, Network center for EANET \(Acid Deposition Monitoring](#)
772 [Network in East Asia\), Nigata, Japan, 2011.](#)

773 [EANET: Data Report 2011, Network center for EANET \(Acid Deposition Monitoring](#)
774 [Network in East Asia\), Nigata, Japan, 2012.](#)

775 [Fang, Y., Koba, K., Makabe, A., Takahashi, C., Zhu, W., Hayashi, T., Hokari, A. A.,](#)
776 [Urakawa, R., Bai, E., Houlton, B. Z., Xi, D., Zhang, S., Matsushita, K., Tu, Y., Liu,](#)
777 [D., Zhu, F., Wang, Z., Zhou, G., Chen, D., Makita, T., Toda, H., Liu, X., Chen, Q.,](#)
778 [Zhang, D., Li, Y. and Yoh, M.: Microbial denitrification dominates nitrate losses from](#)
779 [forest ecosystems, Proc. Natl. Acad. Sci. U. S. A., 112\(5\), 1470–1474,](#)
780 [doi:10.1073/pnas.1416776112, 2015.](#)

781 Galloway, J. N., Aber, J. D., Erisman, J. W., Seitzinger, S. P., Howarth, R. W.,
782 Cowling, E. B. and Cosby, B. J.: The nitrogen cascade, *Bioscience*, 53(4), 341–356,
783 doi:10.1641/0006-3568(2003)053[0341:TNC]2.0.CO;2, 2003.

784 Hattori, S., Nuñez Palma, Y., Itoh, Y., Kawasaki, M., Fujihara, Y., Takase, K. and
785 Yoshida, N.: Isotopic evidence for seasonality of microbial internal nitrogen cycles in
786 a temperate forested catchment with heavy snowfall, *Sci. Total Environ.*, 690, 290–
787 299, doi:10.1016/j.scitotenv.2019.06.507, 2019.

788 Hirota, A., Tsunogai, U., Komatsu, D. D. and Nakagawa, F.: Simultaneous
789 determination of $\delta^{15}\text{N}$ and $\delta^{18}\text{O}$ of N_2O and $\delta^{13}\text{C}$ of CH_4 in nanomolar quantities from
790 a single water sample, *Rapid Commun. Mass Spectrom.*, 24, 1085–1092,
791 doi:10.1002/rcm.4483, 2010.

792 Hornberger, G. M., Bencala, K. E. and McKnight, D. M.: Hydrological controls on
793 dissolved organic carbon during snowmelt in the Snake River near Montezuma,

794 Colorado, *Biogeochemistry*, 25(3), 147–165, doi:10.1007/BF00024390, 1994.

795 Huang, S., Wang, F., Elliott, E. M., Zhu, F., Zhu, W., Koba, K., Yu, Z., Hobbie, E.

796 A., Michalski, G., Kang, R., Wang, A., Zhu, J., Fu, S. and Fang, Y.: Multiyear

797 Measurements on $\Delta^{17}\text{O}$ of Stream Nitrate Indicate High Nitrate Production in a

798 Temperate Forest, *Environ. Sci. Technol.*, 54(7), 4231–4239,

799 doi:10.1021/acs.est.9b07839, 2020.

800 [Inamdar, S. P. and Mitchell, M. J.: Hydrologic and topographic controls on storm-](#)

801 [event exports of dissolved organic carbon \(BOC\) and nitrate across catchment scales,](#)

802 [Water Resour. Res.](#), 42(3), 1–16, doi:10.1029/2005WR004212, 2006.

803 Inoue, T., Nakagawa, F., Shibata, H. and Tsunogai, U.: Vertical Changes in the Flux

804 of Atmospheric Nitrate From a Forest Canopy to the Surface Soil Based on $\Delta^{17}\text{O}$

805 Values, *J. Geophys. Res. Biogeosciences*, 126(4), 1–18, doi:10.1029/2020JG005876,

806 2021.

807 Kaiser, J., Hastings, M. G., Houlton, B. Z., Röckmann, T. and Sigman, D. M.: Triple

808 oxygen isotope analysis of nitrate using the denitrifier method and thermal

809 decomposition of N_2O , *Anal. Chem.*, 79(2), 599–607, doi:10.1021/ac061022s, 2007.

810 Kamisako, M., Sase, H., Matsui, T., Suzuki, H., Takahashi, A., Oida, T., Nakata, M.,

811 Totsuka, T. and Ueda, H.: Seasonal and annual fluxes of inorganic constituents in a

812 small catchment of a Japanese cedar forest near the sea of Japan, *Water. Air. Soil*

813 *Pollut.*, 195(1–4), 51–61, doi:10.1007/s11270-008-9726-8, 2008.

814 [Kaushal, S. S., Groffman, P. M., Band, L. E., Elliott, E. M., Shields, C. A. and](#)

815 ~~Kendall, C.: Tracking nonpoint source nitrogen pollution in human-impacted-~~
816 ~~watersheds, Environ. Sci. Technol., 45(19), 8225–8232, doi:10.1021/es200779e,~~
817 ~~2011.~~

818 Keeling, D.: The concentration and isotopic abundances of atmospheric carbon
819 dioxide in rural areas, *Geochim. Cosmochim. Acta*, 13, 322–334,
820 doi:[https://doi.org/10.1016/0016-7037\(58\)90033-4](https://doi.org/10.1016/0016-7037(58)90033-4), 1958.

821 Kendall, C., Elliott, E. M. and Wankel, S. D.: Tracing Anthropogenic Inputs of
822 Nitrogen to Ecosystems, *Stable Isot. Ecol. Environ. Sci. Second Ed.*, 375–449,
823 doi:[10.1002/9780470691854.ch12](https://doi.org/10.1002/9780470691854.ch12), 2008.

824 Kotlash, A. R. and Chessman, B. C.: Effects of water sample preservation and storage
825 on nitrogen and phosphorus determinations: Implications for the use of automated
826 sampling equipment, *Water Res.*, 32(12), 3731–3737, doi:10.1016/S0043-
827 1354(98)00145-6, 1998.

828 Komatsu, D. D., Ishimura, T., Nakagawa, F. and Tsunogai, U.: Determination of the
829 $^{15}\text{N}/^{14}\text{N}$, $^{17}\text{O}/^{16}\text{O}$, and $^{18}\text{O}/^{16}\text{O}$ ratios of nitrous oxide by using continuous-flow
830 isotope-ratio mass spectrometry Daisuke, *Rapid Commun. Mass Spectrom.*, 22, 1587–
831 1596, doi:[10.1002/rcm.3493](https://doi.org/10.1002/rcm.3493), 2008.

832 Konno, U., Tsunogai, U., Komatsu, D. D., Daita, S., Nakagawa, F., Tsuda, A.,
833 Matsui, T., Eum, Y. J. and Suzuki, K.: Determination of total N_2 fixation rates in the
834 ocean taking into account both the particulate and filtrate fractions, *Biogeosciences*,
835 7(8), 2369–2377, doi:[10.5194/bg-7-2369-2010](https://doi.org/10.5194/bg-7-2369-2010), 2010.

836 McHale, M. R., McDonnell, J. J., Mitchell, M. J. and Cirimo, C. P.: A field-based
837 study of soil water and groundwater nitrate release in an Adirondack forested
838 watershed, *Water Resour. Res.*, 38(4), 2-1-2-16, doi:10.1029/2000wr000102, 2002.

839 McIlvin, M. R. and Altabet, M. A.: Chemical conversion of nitrate and nitrite to
840 nitrous oxide for nitrogen and oxygen isotopic analysis in freshwater and seawater,
841 *Anal. Chem.*, 77(17), 5589–5595, doi:10.1021/ac050528s, 2005.

842 Michalski, G., Scott, Z., Kabling, M. and Thiemens, M. H.: First measurements and
843 modeling of $\Delta^{17}\text{O}$ in atmospheric nitrate, *Geophys. Res. Lett.*, 30(16), 3–6,
844 doi:10.1029/2003GL017015, 2003.

845 Michalski, G., Meixner, T., Fenn, M., Hernandez, L., Sirulnik, A., Allen, E. and
846 Thiemens, M.: Tracing Atmospheric Nitrate Deposition in a Complex Semiarid
847 Ecosystem Using $\Delta^{17}\text{O}$, *Environ. Sci. Technol.*, 38(7), 2175–2181,
848 doi:10.1021/es034980+, 2004.

849 Mitchell, M. J., Iwatsubo, G., Ohru, K. and Nakagawa, Y.: Nitrogen saturation in
850 Japanese forests: An evaluation, *For. Ecol. Manage.*, 97(1), 39–51,
851 doi:10.1016/S0378-1127(97)00047-9, 1997.

852 Morin, S., Sander, R. and Savarino, J.: Simulation of the diurnal variations of the
853 oxygen isotope anomaly ($\Delta^{17}\text{O}$) of reactive atmospheric species, *Atmos. Chem. Phys.*,
854 11(8), 3653–3671, doi:10.5194/acp-11-3653-2011, 2011.

855 Nakagawa, F., Suzuki, A., Daita, S., Ohyama, T., Komatsu, D. D. and Tsunogai, U.:
856 Tracing atmospheric nitrate in groundwater using triple oxygen isotopes: Evaluation

857 based on bottled drinking water, *Biogeosciences*, 10(6), 3547–3558, doi:10.5194/bg-
858 10-3547-2013, 2013.

859 Nakagawa, F., Tsunogai, U., Obata, Y., Ando, K., Yamashita, N., Saito, T.,
860 Uchiyama, S., Morohashi, M. and Sase, H.: Export flux of unprocessed atmospheric
861 nitrate from temperate forested catchments: A possible new index for nitrogen
862 saturation, *Biogeosciences*, 15(22), 7025–7042, doi:10.5194/bg-15-7025-2018, 2018.

863 Nelson, D. M., Tsunogai, U., Ding, D., Ohyama, T., Komatsu, D. D., Nakagawa, F.,
864 Noguchi, I. and Yamaguchi, T.: Triple oxygen isotopes indicate urbanization affects
865 sources of nitrate in wet and dry atmospheric deposition, *Atmos. Chem. Phys.*, 18(9),
866 6381–6392, doi:10.5194/acp-18-6381-2018, 2018.

867 Ocampo, C. J., Sivapalan, M. and Oldham, C.: Hydrological connectivity of upland-
868 riparian zones in agricultural catchments: Implications for runoff generation and
869 nitrate transport, *J. Hydrol.*, 331(3–4), 643–658, doi:10.1016/j.jhydrol.2006.06.010,
870 2006.

871 Ohte, N., Sebestyen, S. D., Shanley, J. B., Doctor, D. H., Kendall, C., Wankel, S. D.
872 and Boyer, E. W.: Tracing sources of nitrate in snowmelt runoff using a high-
873 resolution isotopic technique, *Geophys. Res. Lett.*, 31(21), 2–5,
874 doi:10.1029/2004GL020908, 2004.

875 Ohte, N., Tayasu, I., Kohzu, A., Yoshimizu, C., Osaka, K., Makabe, A., Koba, K.,
876 Yoshida, N. and Nagata, T.: Spatial distribution of nitrate sources of rivers in the lake
877 Biwa Watershed, Japan: Controlling factors revealed by nitrogen and oxygen isotope

878 values, *Water Resour. Res.*, 46(7), 1–16, doi:10.1029/2009WR007871, 2010.

879 Paerl, H. W. and Huisman, J.: Climate change: A catalyst for global expansion of
880 harmful cyanobacterial blooms, *Environ. Microbiol. Rep.*, 1(1), 27–37,
881 doi:10.1111/j.1758-2229.2008.00004.x, 2009.

882 Pellerin, B. A., Saraceno, J. F., Shanley, J. B., Sebestyen, S. D., Aiken, G. R.,
883 Wollheim, W. M. and Bergamaschi, B. A.: Taking the pulse of snowmelt: In situ
884 sensors reveal seasonal, event and diurnal patterns of nitrate and dissolved organic
885 matter variability in an upland forest stream, *Biogeochemistry*, 108(1–3), 183–198,
886 doi:10.1007/s10533-011-9589-8, 2012.

887 Peterjohn, W. T., Adams, M. B. and Gilliam, F. S.: Symptoms of nitrogen saturation
888 in two central Appalachian hardwood forest ecosystems, *Biogeochemistry*, 35(3),
889 507–522, doi:10.1007/BF02183038, 1996.

890 Piatek, K. B., Mitchell, M. J., Silva, S. R. and Kendall, C.: Sources of nitrate in
891 snowmelt discharge: Evidence from water chemistry and stable isotopes of nitrate,
892 *Water. Air. Soil Pollut.*, 165(1–4), 13–35, doi:10.1007/s11270-005-4641-8, 2005.

893 Riha, K. M., Michalski, G., Gallo, E. L., Lohse, K. A., Brooks, P. D. and Meixner, T.:
894 High Atmospheric Nitrate Inputs and Nitrogen Turnover in Semi-arid Urban
895 Catchments, *Ecosystems*, 17(8), 1309–1325, doi:10.1007/s10021-014-9797-x, 2014.

896 Rose, L. A., Elliott, E. M. and Adams, M. B.: Triple Nitrate Isotopes Indicate
897 Differing Nitrate Source Contributions to Streams Across a Nitrogen Saturation
898 Gradient, *Ecosystems*, 18(7), 1209–1223, doi:10.1007/s10021-015-9891-8, 2015.

899 Sabo, R. D., Nelson, D. M. and Eshleman, K. N.: Episodic, seasonal, and annual
900 export of atmospheric and microbial nitrate from a temperate forest, *Geophys. Res.*
901 *Lett.*, 43(2), 683–691, doi:10.1002/2015GL066758, 2016.

902 Sase, H., Takahashi, A., Sato, M., Kobayashi, H., Nakata, M. and Totsuka, T.:
903 Seasonal variation in the atmospheric deposition of inorganic constituents and canopy
904 interactions in a Japanese cedar forest, *Environ. Pollut.*, 152(1), 1–10,
905 doi:10.1016/j.envpol.2007.06.023, 2008.

906 Sase, H., Saito, T., Takahashi, M., Morohashi, M., Yamashita, N., Inomata, Y.,
907 Ohizumi, T. and Nakata, M.: Transboundary air pollution reduction rapidly reflected
908 in stream water chemistry in forested catchment on the Sea of Japan coast in central
909 Japan, *Atmos. Environ.*, 248(November 2020), 118223,
910 doi:10.1016/j.atmosenv.2021.118223, 2021.

911 [Sebestyen, S. D., Ross, D. S., Shanley, J. B., Elliott, E. M., Kendall, C., Campbell, J.](#)
912 [L., Dail, D. B., Fernandez, I. J., Goodale, C. L., Lawrence, G. B., Lovett, G. M.,](#)
913 [McHale, P. J., Mitchell, M. J., Nelson, S. J., Shattuck, M. D., Wickman, T. R.,](#)
914 [Barnes, R. T., Bostic, J. T., Buda, A. R., Burns, D. A., Eshleman, K. N., Finlay, J. C.,](#)
915 [Nelson, D. M., Ohte, N., Pardo, L. H., Rose, L. A., Sabo, R. D., Schiff, S. L.,](#)
916 [Spoelstra, J. and Williard, K. W. J.: Unprocessed Atmospheric Nitrate in Waters of](#)
917 [the Northern Forest Region in the U.S. and Canada, *Environ. Sci. Technol.*, 53\(7\),](#)
918 [3620–3633, doi:10.1021/acs.est.9b01276, 2019.](#)

919 [Sebestyen, S. D., Shanley, J. B., Boyer, E. W., Kendall, C. and Doctor, D. H.:](#)

920 ~~Coupled hydrological and biogeochemical processes controlling variability of~~
921 ~~nitrogen species in streamflow during autumn in an upland forest, , 1569–1591,~~
922 ~~doi:10.1002/2013WR013670, 2014.~~

923 Stoddard, J. L.: Long-Term Changes in Watershed Retention of Nitrogen, , 223–284,
924 doi:10.1021/ba-1994-0237.ch008, 1994.

925 Tsunogai, U., Komatsu, D. D., Daita, S., Kazemi, G. A., Nakagawa, F., Noguchi, I.
926 and Zhang, J.: Tracing the fate of atmospheric nitrate deposited onto a forest
927 ecosystem in Eastern Asia using $\Delta^{17}\text{O}$, *Atmos. Chem. Phys.*, 10(4), 1809–1820,
928 doi:10.5194/acp-10-1809-2010, 2010.

929 Tsunogai, U., Daita, S., Komatsu, D. D., Nakagawa, F. and Tanaka, A.: Quantifying
930 nitrate dynamics in an oligotrophic lake using $\Delta^{17}\text{O}$, *Biogeosciences*, 8(3), 687–702,
931 doi:10.5194/bg-8-687-2011, 2011.

932 Tsunogai, U., Komatsu, D. D., Ohyama, T., Suzuki, A., Nakagawa, F., Noguchi, I.,
933 Takagi, K. and Nomura, M.: Quantifying the effects of clear-cutting and strip-cutting
934 on nitrate dynamics in a forested watershed using triple oxygen isotopes as tracers, ,
935 (1), 5411–5424, doi:10.5194/bg-11-5411-2014, 2014.

936 Tsunogai, U., Miyauchi, T., Ohyama, T., Komatsu, D. D., Nakagawa, F., Obata, Y.,
937 Sato, K. and Ohizumi, T.: Accurate and precise quantification of atmospheric nitrate
938 in streams draining land of various uses by using triple oxygen isotopes as tracers,
939 *Biogeosciences*, 13(11), 3441–3459, doi:10.5194/bg-13-3441-2016, 2016.

940 Tsunogai, U., Miyauchi, T., Ohyama, T., Komatsu, D. D., Ito, M. and Nakagawa, F.:

941 Quantifying nitrate dynamics in a mesotrophic lake using triple oxygen isotopes as
942 tracers, *Limnol. Oceanogr.*, 63, S458–S476, doi:10.1002/lno.10775, 2018.

943 Vitousek, P. M. and Howarth, R. W.: Nitrogen limitation on land and in the sea: How
944 can it occur?, *Biogeochemistry*, 13(2), 87–115, doi:10.1007/BF00002772, 1991.

945 Yamazaki, A., Watanabe, T. and Tsunogai, U.: Nitrogen isotopes of organic nitrogen
946 in reef coral skeletons as a proxy of tropical nutrient dynamics, *Geophys. Res. Lett.*,
947 38(19), 1–5, doi:10.1029/2011GL049053, 2011.